NATIONAL ADVISORY COMMITTEE FOR AERONAUTICS

REPORT No. 581

MEASUREMENTS OF INTENSITY AND SCALE OF WIND-TUNNEL TURBULENCE AND THEIR RELATION TO THE CRITICAL REYNOLDS NUMBER OF SPHERES

By HUGH L. DRYDEN, G. B. SCHUBAUER, W. C. MOCK, Jr.
and H. K. SKRAMSTAD

1937

For sale by the Superintendent of Documents, Washington, D. C. - - - - - - - - - - - - - - - Price 15 cents

AERONAUTIC SYMBOLS

1. FUNDAMENTAL AND DERIVED UNITS

	Symbol	Metric		English	
		Unit	Abbreviation	Unit	Abbreviation
Length	l	meter	m	foot (or mile)	ft. (or mi.)
Time	t	second	s	second (or hour)	sec. (or hr.)
Force	F	weight of 1 kilogram	kg	weight of 1 pound	lb.
Power	P	horsepower (metric)		horsepower	hp.
Speed	V	kilometers per hour	k.p.h.	miles per hour	m.p.h.
		meters per second	m.p.s.	feet per second	f.p.s.

2. GENERAL SYMBOLS

W, Weight $= mg$

g, Standard acceleration of gravity = 9.80665 m/s^2 or 32.1740 ft./sec.^{2}

m, Mass $= \frac{W}{g}$

I, Moment of inertia $= mk^2$. (Indicate axis of radius of gyration k by proper subscript.)

μ, Coefficient of viscosity

ν, Kinematic viscosity

ρ, Density (mass per unit volume)

Standard density of dry air, 0.12497 kg-m^{-4}-s^2 at 15° C. and 760 mm; or 0.002378 lb.-ft.$^{-4}$-sec.^{2}

Specific weight of "standard" air, 1.2255 kg/m^3 or 0.07651 lb./cu.ft.

3. AERODYNAMIC SYMBOLS

S, Area

S_w, Area of wing

G, Gap

b, Span

c, Chord

$\frac{b^2}{S}$, Aspect ratio

V, True air speed

q, Dynamic pressure $= \frac{1}{2}\rho V^2$

L, Lift, absolute coefficient $C_L = \frac{L}{qS}$

D, Drag, absolute coefficient $C_D = \frac{D}{qS}$

D_o, Profile drag, absolute coefficient $C_{D_o} = \frac{D_o}{qS}$

D_i, Induced drag, absolute coefficient $C_{D_i} = \frac{D_i}{qS}$

D_p, Parasite drag, absolute coefficient $C_{D_p} = \frac{D_p}{qS}$

C, Cross-wind force, absolute coefficient $C_C = \frac{C}{qS}$

R, Resultant force

i_w, Angle of setting of wings (relative to thrust line)

i_t, Angle of stabilizer setting (relative to thrust line)

Q, Resultant moment

Ω, Resultant angular velocity

$\frac{Vl}{\rho}{\mu}$, Reynolds Number, where l is a linear dimension (e.g., for a model airfoil 3 in. chord, 100 m.p.h. normal pressure at 15° C., the corresponding number is 234,000; or for a model of 10 cm chord, 40 m.p.s. the corresponding number is 274,000)

C_p, Center-of-pressure coefficient (ratio of distance of $c.p.$ from leading edge to chord length)

α, Angle of attack

ϵ, Angle of downwash

α_o, Angle of attack, infinite aspect ratio

α_i, Angle of attack, induced

α_a, Angle of attack, absolute (measured from zero-lift position)

γ, Flight-path angle

REPORT No. 581

MEASUREMENTS OF INTENSITY AND SCALE OF WIND-TUNNEL TURBULENCE AND THEIR RELATION TO THE CRITICAL REYNOLDS NUMBER OF SPHERES

By HUGH L. DRYDEN, G. B. SCHUBAUER, W. C. MOCK, Jr.
and H. K. SKRAMSTAD
National Bureau of Standards

112108—37——1

NATIONAL ADVISORY COMMITTEE FOR AERONAUTICS

HEADQUARTERS, NAVY BUILDING, WASHINGTON, D. C.

LABORATORIES, LANGLEY FIELD, VA.

Created by act of Congress approved March 3, 1915, for the supervision and direction of the scientific study of the problems of flight (U. S. Code, Title 50, Sec. 151). Its membership was increased to 15 by act approved March 2, 1929. The members are appointed by the President, and serve as such without compensation.

TECHNICAL COMMITTEES

AERODYNAMICS
POWER PLANTS FOR AIRCRAFT
AIRCRAFT STRUCTURES AND MATERIALS

AIRCRAFT ACCIDENTS
INVENTIONS AND DESIGNS

Coordination of Research Needs of Military and Civil Aviation

Preparation of Research Programs

Allocation of Problems

Prevention of Duplication

Consideration of Inventions

LANGLEY MEMORIAL AERONAUTICAL LABORATORY

LANGLEY FIELD, VA.

Unified conduct, for all agencies, of scientific research on the fundamental problems of flight.

OFFICE OF AERONAUTICAL INTELLIGENCE

WASHINGTON, D. C.

Collection classification, compilation, and dissemination of scientific and technical information on aeronautics.

REPORT No. 581

MEASUREMENTS OF INTENSITY AND SCALE OF WIND-TUNNEL TURBULENCE AND THEIR RELATION TO THE CRITICAL REYNOLDS NUMBER OF SPHERES

By Hugh L. Dryden, G. B. Schubauer, W. C. Mock, Jr., and H. K. Skramstad

SUMMARY

The investigation of wind-tunnel turbulence, conducted at the National Bureau of Standards with the cooperation and financial assistance of the National Advisory Committee for Aeronautics, has been extended to include a new variable, namely, the scale of the turbulence. This new variable has been studied together with the intensity of the turbulence, and the effect of both on the critical Reynolds Number of spheres has been investigated.

By the use of a modification of the usual hot-wire apparatus incorporating two hot wires suitably connected and mounted so that the cross-stream distance between them may be varied, it has been found possible to determine the correlation between the speed fluctuations existing at the two wires. If u_1 and u_2 are the velocity fluctuations in the direction of the mean speed at the first and second wires, respectively, a correlation coefficient $R(y)$, equal to $\frac{\overline{u_1 u_2}}{\sqrt{\overline{u_1^2}}\sqrt{\overline{u_2^2}}}$ may be found as a function of the separation y. A length characterizing the scale of the turbulence may then be defined by the relation—

$$L=\int_0^\infty R(y)dy$$

The intensity of the turbulence as given by $\frac{\sqrt{\overline{u^2}}}{U}$, where U is the average speed of the stream, and the quantity L were determined by measurements in an air stream made turbulent to various degrees by screens of various mesh. The value of L near the screen was found to be about the same as the wire size of the screen, but increased with distance downstream from the screen. The quantity L may be regarded as a rough measure of the size of the eddies shed by the wires of the screen. The intensity was found to decrease with distance in accordance with the law of decay derived by G. I. Taylor.

Hot-wire measurements of turbulence are in error where the quantity L is of the same order as the length of the wire used. In the present work corrections for the lack of correlation over the entire length of the wires have been made in the measured values of L and $\frac{\sqrt{\overline{u^2}}}{U}$.

With both L and $\frac{\sqrt{\overline{u^2}}}{U}$ known for the stream with the several screens, the critical Reynolds Numbers of spheres were investigated. It was found that the critical Reynolds Number depended on $\frac{D}{L}$, where D is the diameter of the sphere, as well as on $\frac{\sqrt{\overline{u^2}}}{U}$; and that a functional relation between the critical Reynolds Number and $\frac{\sqrt{\overline{u^2}}}{U}\left(\frac{D}{L}\right)^{\frac{1}{5}}$ suggested by G. I. Taylor, was satisfied to within the experimental uncertainty. It is shown that the effect of the size of the sphere that has been observed by other investigators is but a particular manifestation of the foregoing more general relation.

INTRODUCTION

The turbulence of the air stream is generally recognized as a variable of considerable importance in many aerodynamic phenomena, especially those observed in wind tunnels. The drag of an airship model may vary by a factor of 2, the drag of a sphere by a factor of 4, and the maximum lift of an airfoil by a factor of 1.3 in air streams of different turbulence. The determination of turbulence is now a routine matter in many wind tunnels, the most common method being that of determining the value of the Reynolds Number of a sphere for which the drag coefficient is 0.3, the so-called critical Reynolds Number.

The critical Reynolds Number of a sphere is a measure of the aerodynamic effect of turbulence on a particular body and not a direct measurement of the turbulence. A direct measurement of the intensity of the turbulence can be made by means of a hot-wire anemometer suitably compensated for the lag of the wire (reference 1). The intensity of the turbulence is defined as the ratio of the root-mean-square speed fluctuation at a point to the mean speed. The experiments described in reference 1, (fig. 7), show a good correlation between the intensity of the turbulence and the critical Reynolds Numbers of spheres. In subsequent work at the National Bureau of Standards (reference 2) in which various honeycombs were used in the same wind tunnel and the entrance cone was modified, the correlation was not nearly so good.

The existence of a fair correlation was confirmed by Millikan and Klein at the California Institute of Technology (reference 3). These investigators noted that

the critical Reynolds Number of the sphere depended to some extent on the diameter of the sphere, decreasing as the diameter increased.

Since the critical Reynolds Number occurs at lower speeds for larger diameters, it might be supposed that the variation of the critical Reynolds Number with diameter really indicated a variation of the intensity of the turbulence with speed. The direct measurements of the intensity by the hot-wire anemometer show, however, that this explanation cannot be correct. We are thus led to the idea that the scale of the turbulent pattern must be considered. In fact, as early as 1923, Bacon and Reid, in reference 4, predicted an effect of the scale or "grain" of the turbulence and stated that the "effect of scale of turbulence is to control the degree with which true dynamic similarity may be maintained throughout a series of tests with spheres of different size." A study of this subject was begun at the National Bureau of Standards in the fall of 1933.

In order to investigate experimentally the effect of scale of the turbulence as well as its intensity, measurements of the critical Reynolds Number of spheres were made in a stream rendered turbulent by screens of various mesh. The investigation was conducted in the 4½-foot wind tunnel, the screens being placed one at a time completely across the upstream working section of the tunnel. In all, five nearly similar square-mesh screens were used, ranging in size from a 5-inch mesh made of round rods 1 inch in diameter to a ¼-inch mesh with a wire diameter of 0.05 inch. The purpose of the several screens was to vary the scale of the turbulence, it being supposed that the scale would be proportional to the mesh of the screen. It was decided subsequently to measure some dimension characteristic of the fluctuations themselves, and the dimension chosen was that derived from measurements of the correlation between velocity fluctuations at points at varying distances apart transverse to the stream.

Values of the intensity of the turbulence measured by the hot-wire method at different distances downstream from the several screens showed that the turbulence decayed rapidly at first and then more slowly with increasing distance from the screens. Hence in the sphere measurements the intensity of the turbulence produced by any one screen could be varied by varying the distance between the sphere and the screen.

As may be seen from the foregoing discussion, the complete program included several problems, which are treated in the five separate parts of the report as outlined below:

I. The measurement of correlation between velocity fluctuations with modified hot-wire equipment, and the derivation of a length to define the scale of the turbulence, by G. B. Schubauer, W. C. Mock, Jr., and H. K. Skramstad.

II. Measurements of the intensity and rate of decay of turbulence employing the usual type of hot-wire equipment, by G. B. Schubauer, W. C. Mock, Jr., and H. K. Skramstad.

III. The determination of the critical Reynolds Number of spheres under conditions where both the intensity and the scale of the turbulence are known, by Hugh L. Dryden, G. B. Schubauer, and W. C. Mock, Jr.

IV. The mathematical theory pertaining to the correction of the measurements, both of scale and intensity, for lack of complete correlation of the fluctuations over the entire length of the wires, by H. K. Skramstad.

V. Certain subsidiary matters relating to the variation of the correlation coefficient with the frequency characteristics of the measuring apparatus and with azimuth, by Hugh L. Dryden, G. B. Schubauer, and W. C. Mock, Jr.

Throughout the later stages of the work, the staff has been fortunate in being able to discuss by correspondence various aspects of the problem with G. I. Taylor, of Cambridge, England. The discussion of the experimental results is given in terms of his statistical theory of turbulence outlined in reference 5.

I—THE SCALE OF TURBULENCE AS DERIVED FROM MEASUREMENTS OF CORRELATION BETWEEN VELOCITY FLUCTUATIONS

When air flows past guide vanes or straighteners, such as those commonly used in wind tunnels either separately or in the form of a honeycomb, a considerable amount of eddy motion is set up and is carried along with the stream making the flow turbulent. Guide vanes are necessary to prevent large and erratic speed fluctuations, which would exist in the absence of the vanes, as well as to guide the air around turns. It may be assumed as a rough approximation that the eddy size and hence the scale of the turbulence is controlled by some dimension characteristic of the size or the arrangement of the guide vanes. For the case where the guide vanes are arranged in the form of a honeycomb, G. I. Taylor (reference 5) has assumed that the scale of the turbulence is proportional to the size of the cells of the honeycomb.

Figure 1 shows a sketch of the 4-½-foot tunnel used in the present work, in which a honeycomb (B) of 4-inch cells was located at the extreme entrance end and was followed by a contraction in diameter from 10 feet at the honeycomb to 4-½ feet at the working section. Owing to the rather rapid decay of eddy motion, the turbulence always decreases in intensity with distance from its source. In the working section of the present tunnel the intensity of the turbulence was 0.85 percent.[1] The law of eddy decay and the factors governing the scale of the turbulence will be taken up in detail in later sections.

In order to vary the two quantities, intensity and scale, the five screens listed in table I were placed indi-

[1] This is the value corrected for the effect of the length of the wire used in the measurement. The uncorrected value as observed with a wire 8.4 millimeters long was 0.7 percent.

vidually across the upstream working section of the tunnel at the position indicated in figure 1. Figure 2 shows photographs of a small portion of each of the screens, illustrating their relative size and type of construction. It is quite evident that the stream will be rendered turbulent by the eddies shed from a given screen and that the initial size of the eddies, and hence the scale of the turbulence near its point of origin, will be determined by some dimension of the screen. An effort was made to obtain screens of uniform mesh and wire size and to have the five screens as nearly similar to one another as possible. It will be seen by the variations in dimensions shown in table I and by the difference in type of construction shown in figure 2 that neither condition was exactly fulfilled. Since the deviations from the nominal size found by comparing columns 1 and 2 in table I are not outside the average deviations

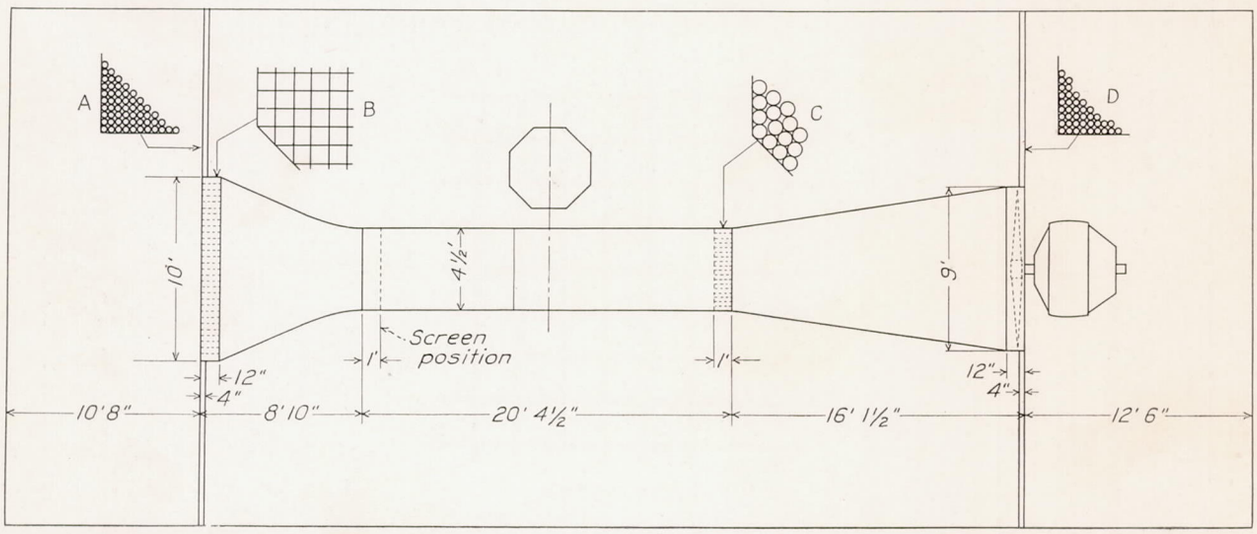

FIGURE 1.—Diagram of the wind tunnel showing position of screens and length of working section. A and D: paper tubes—1 in. diameter, 4 in. long, 3/32 in. wall. B: wooden cells—4 in. square, 12 in. long, 5/16 in. wall. C: metal tubes—3 inch diameter, 12 in. long, 0.025 in. wall.

of the individual meshes from the mean, the nominal mesh size was used as the length characteristic of the screen.

It will appear later that the scale of the turbulence near a screen corresponds more nearly to the wire size than to the mesh size. This fact should not be construed to indicate that the wire size determines the scale since the correspondence depends on the way in which the scale is defined. Since the screens may be regarded as geometrically similar, it is immaterial whether the size of the screen is specified by the wire size or the mesh size.

Immediately downstream from the screens the wakes of the individual wires or rods caused the air speed and the turbulence to vary with position across stream. However at distances greater than 15 mesh lengths the regular pattern of the screen was found to have disappeared, leaving the average speed approximately uniform and the turbulence nearly uniformly distributed. The uniformity of the stream will be discussed at greater length in connection with the sphere measurements in part III.

HOT-WIRE EQUIPMENT USED IN TURBULENCE MEASUREMENTS

A brief description of the essential features of the hot wire and its application to studies of turbulence will suffice here, since full accounts dealing with such equipment may be found in the literature, notably in references 1, 6, and 7. Fundamentally the apparatus consists of a particular type of hot-wire anemometer with an electrically heated wire of such small diameter that the speed fluctuations of the stream in which the wire is placed will cause changes in the wire temperature. The fluctuating voltage drop across the wire, accompanying temperature and resistance changes, would serve as an indication of the speed fluctuations were it not for the failure of the wire to follow the faster fluctuations because of the lag introduced by its thermal capacity. It is however, possible to compensate for this characteristic of the wire by means of an electric network containing an inductance and resistance having the opposite effect. The voltage output of the wire is usually amplified before compensation is introduced, and then the compensated voltage is given additional amplification to enable it to be measured. The indicator used in the present work was a thermal type milliammeter connected to the output of the amplifier. This instrument indicated the mean square of the alternating current output of the amplifier and, with the amplifier calibrated against a known input voltage, the meter reading could be used to calculate the mean square of the compensated voltage fluctuation. In addition, the direct voltage drop across the wire was measured by a potentiometer. All the information necessary for calculating the root-mean-square of the speed fluctuation was thus made available. Details of such calculations are given in reference 1. The factors on which com

pensation depends and the formula for computing the compensation are given in reference 6.

The amplifier used in the present work was not the one described in reference 7, a new amplifier of a similar type having since been built to make possible the use of an alternating current power supply. The frequency characteristics of both the old and the new amplifiers, when combined with the compensating circuit were such as to give satisfactory compensation to all frequencies from a few cycles per second to about 1,000 cycles per second. The platinum wire used in the present work was 0.016 millimeter in diameter; the length was usually 5 millimeters, although some older results are given for which the wire length was 8.4 millimeters.

If the turbulence is isotropic, as it will later be shown to be at a sufficient distance from the source of the disturbance, the fluctuations have equal velocity components in all directions. It is usual, however, to interpret the measured velocity fluctuations as being made up wholly of the component u in the direction of the mean speed and to neglect entirely the normal component v. The justification for doing so lies in the fact that the v component when superposed on the mean speed has a very much smaller effect on the cooling of the wire than a u component of the same magnitude. The intensity of the turbulence is therefore expressed in terms of $\frac{\sqrt{\overline{u^2}}}{U}$, where $\sqrt{\overline{u^2}}$ is the root-mean-square of the

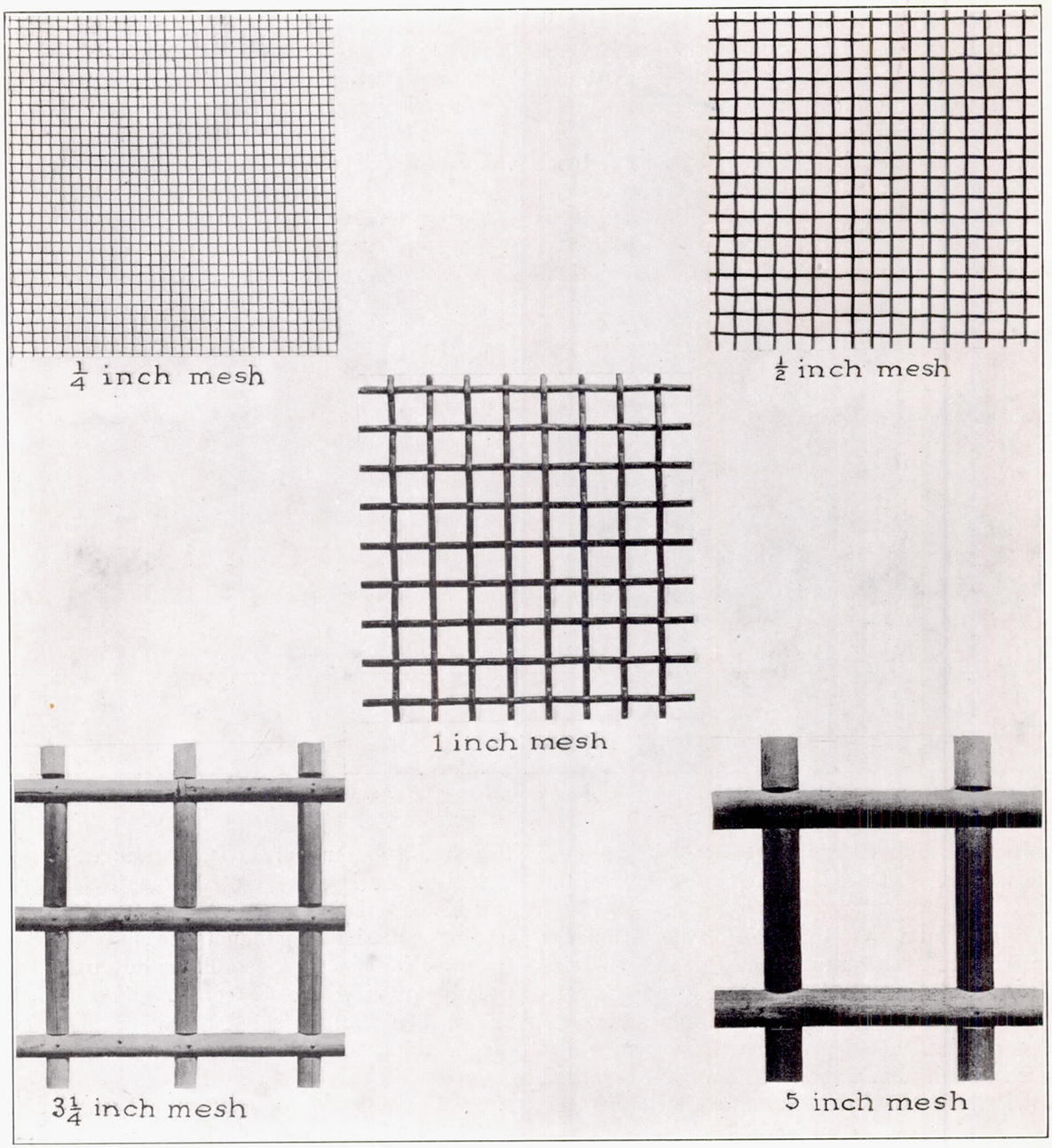

FIGURE 2.—The screens used to produce turbulence showing relative size and type of construction.

u component of the fluctuations and U is the average speed. The term "percentage turbulence" is commonly used to denote $100\,\frac{\sqrt{\overline{u^2}}}{U}$.

APPLICATION OF HOT-WIRE EQUIPMENT TO CORRELATION MEASUREMENTS

The determination of the scale of the turbulence involved a procedure closely related to that just described since the length characterizing the scale could best be derived from the distance transverse to the stream over which correlation existed between velocity fluctuations. It was therefore desired to obtain the correlation between the velocity fluctuations at two points separated by known distances across the stream and to express this correlation in terms of the conventional correlation coefficient

$$R=\frac{\overline{u_1u_2}}{\sqrt{\overline{u_1^2}}\sqrt{\overline{u_2^2}}}$$

where u_1 and u_2 are the velocity fluctuations at the points 1 and 2, respectively. The bars signifiy average values. In general, R will be a function $R(y)$ of the separation of the two points, where y is the distance between the points transverse to the stream. It was decided to adopt as a measure of the scale of the turbulence a length L defined as

$$L=\int_0^\infty R(y)dy$$

A length so defined is in accordance with the convention adopted by G. I. Taylor in reference 5.

The experimental problem therefore resolved itself into the determination of the correlation between velocity fluctuations by means of two hot wires. By way of illustrating the method, let us assume two identical wires heated to the same average temperature and placed parallel to one another at a given distance apart. If e_1 and e_2 are the instantaneous values of the fluctuating voltage over the two wires separately, the drop across the two, when they are connected so that their voltages oppose one another, is (e_1-e_2). When the resultant voltage is fed into an amplifier, the indications given by a thermal type milliammeter in the output of the amplifier will be proportional to $\overline{(e_1-e_2)^2}$, where the bar signifies that the meter indicates the average. If compensation is introduced to correct for the attenuation of the higher frequency fluctuations by the wire, then e_1 and e_2 become proportional to u_1 and u_2, the velocity fluctuations at the two wires,[2] and the resultant meter reading will be proportional to $\overline{(u_1-u_2)^2}$.

By the same reasoning it may be seen that a meter reading proportional to $\overline{(u_1+u_2)^2}$ is obtained if the wires are connected so that their voltages add. Figure 3 is a diagram of the electric circuit which shows, in addition to the heating circuits, two sets of potential leads running from the wires to the switch AB by means of which the potentials from the wires may be either added or opposed. If M_a is the meter reading obtained when the voltages are added and M_b is the reading when opposed, then

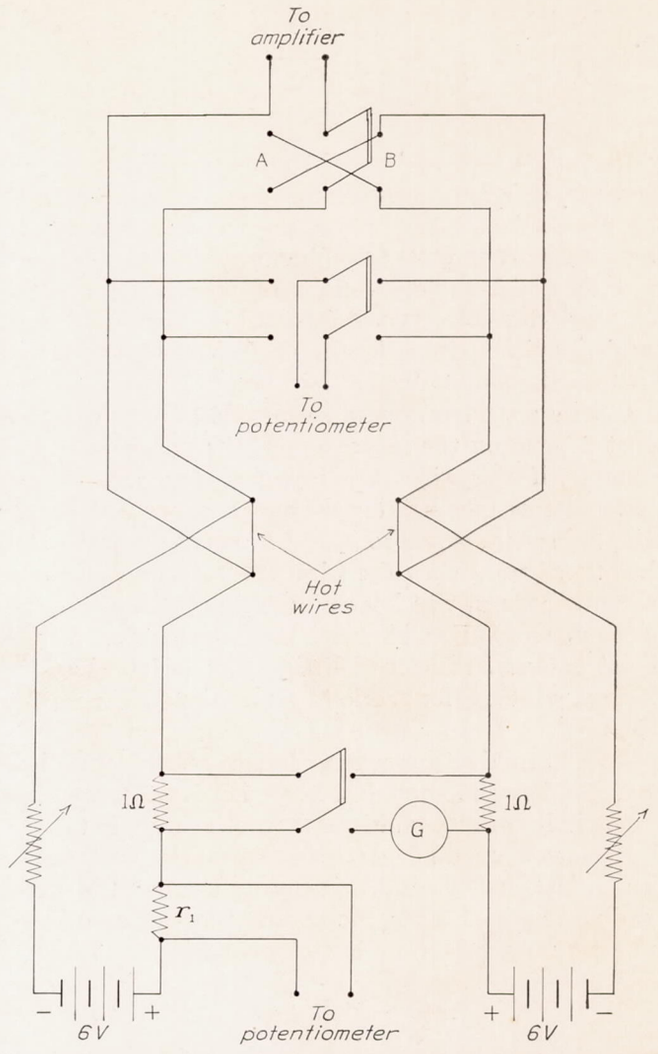

FIGURE 3.—Diagram of the circuit used in the measurement of correlation between velocity fluctuations.

$$M_a=K\overline{(u_1+u_2)^2}=K(\overline{u_1^2}+\overline{u_2^2}+2\overline{u_1u_2}) \quad (1)$$

$$M_b=K\overline{(u_1-u_2)^2}=K(\overline{u_1^2}+\overline{u_2^2}-2\overline{u_1u_2}) \quad (2)$$

where K is simply the constant of proportionality. Forming M_a-M_b and M_a+M_b and dividing

$$\frac{M_a-M_b}{M_a+M_b}=\frac{2\overline{u_1u_2}}{\overline{u_1^2}+\overline{u_2^2}} \quad (3)$$

If the turbulence is uniformly distributed across the stream so that the average square of the fluctuations is the same at wires 1 and 2, then $\overline{u_1^2}=\overline{u_2^2}=\overline{u^2}$, and equation (3) becomes

$$\frac{M_a-M_b}{M_a+M_b}=\frac{\overline{u_1u_2}}{\overline{u^2}} \quad (4)$$

[2] The voltage fluctuations are proportional to the velocity fluctuations only when the latter are small. This condition was closely fulfilled for the conditions of the present experiments.

Under such conditions it is evident that

$$\frac{\overline{u_1u_2}}{\overline{u^2}}=\frac{\overline{u_1u_2}}{\sqrt{\overline{u_1^2}}\sqrt{\overline{u_2^2}}}$$

which is the conventional correlation coefficient. Since, however, it is only possible to measure the average of the fluctuations along wires, the lengths of which in the present case were 5 millimeters, u_1 and u_2 cannot be interpreted as fluctuations at points. Hence the observed correlation coefficient will be denoted by R' as distinguished from R, the coefficient of correlation between the fluctuations at two points.

A little consideration will show that the correlation must depend on the separation of the two wires. For example, if the wires are brought close together so that a disturbance striking the one must strike the other also, u_1 becomes equal to u_2 and R' equal to unity. On the other hand, when the wires are very far apart, the instantaneous u_1 will bear no relation to the instantaneous u_2, and $\overline{u_1u_2}$ and hence R' will equal zero. Values of R' between these two limits may be obtained by taking readings for various separations of the two wires.

An alternative procedure found more convenient than the foregoing one, but less exact if the turbulence is not uniform or conditions are not steady, is to take only meter reading M_b corresponding to various separations of the wires. Denoting by M_b^{∞} the meter reading obtained when the wires are so far apart that no correlation exists, we have by equation (2)

$$M_b^{\infty}=K(\overline{u_1^2}+\overline{u_2^2})$$

Forming the quotient

$$\frac{M_b}{M_b^{\infty}}=\frac{\overline{u_1^2}+\overline{u_2^2}-2\overline{u_1u_2}}{\overline{u_1^2}+\overline{u_2^2}}=1-\frac{2\overline{u_1u_2}}{\overline{u_1^2}+\overline{u_2^2}}$$

and, as before, when $\overline{u_1^2}=\overline{u_2^2}=\overline{u^2}$

$$1-\frac{M_b}{M_b^{\infty}}=\frac{\overline{u_1u_2}}{\overline{u^2}}=R'$$

Obviously M_a could have been used alone in a similar manner but, since M_a does not approach zero for a correlation of unity as does M_b, this method was less sensitive and was never used.

In the wiring diagram of figure 3 the potentiometer and amplifier circuits are omitted since these are standard pieces of equipment. It will be observed that two separate heating circuits are used, the separation of the two circuits being convenient to allow the potential drops across the wires to be either added or opposed. After the current in one of the circuits was set equal to the desired value of 0.2 ampere, as determined by the potentiometer and standard resistance r_1, the current in the other heating circuit was set to the same value by making the drop across the 1 ohm standard resistance in this circuit equal to that across the 1 ohm standard resistance in the other circuit. The potentiometer was also used to measure the voltage drop across each wire. From the voltage drop, the current, and the temperature coefficient of resistance, the temperature of the wire could be computed, a quantity required to compute the compensation resistance.

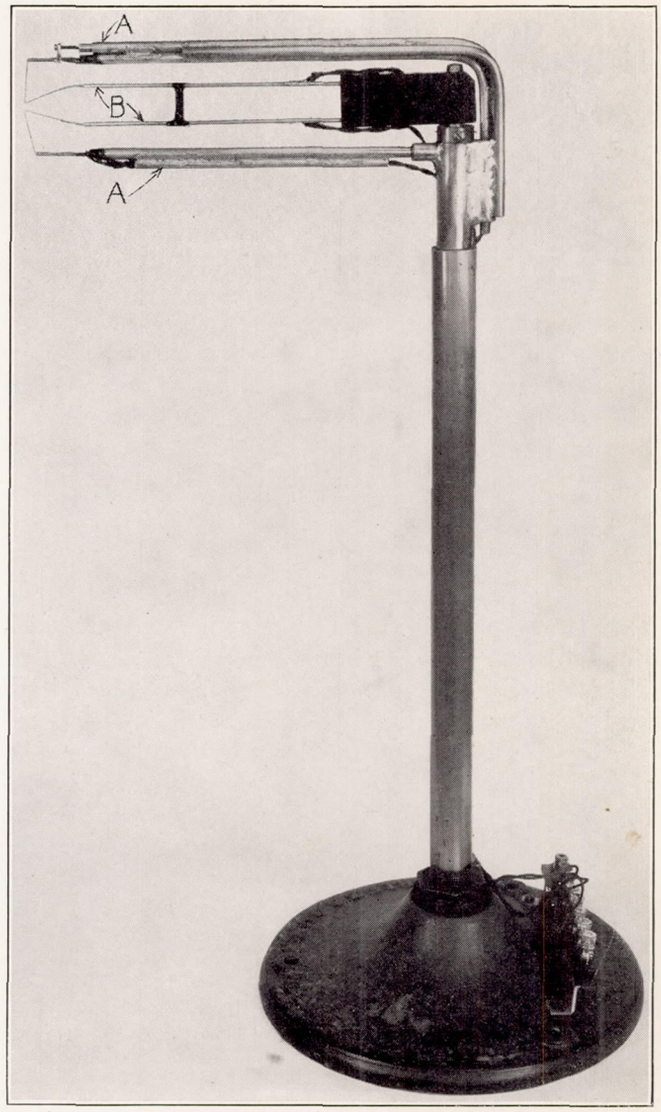

FIGURE 4.—The traversing apparatus used to vary the distance between hot wires in the measurement of correlation between velocity fluctuations.

By means of the traversing apparatus shown in figure 4, the distance between the wires could be varied and R' measured as a function of the distance. The side view of the apparatus clearly shows the two sets of prongs each 1 foot in length from the support to the needle tips to which the wires were attached. The outer set A is fixed rigidly to the vertical supporting member while the inner set B, to permit rotation, is fixed to a vertical shaft running down through the supporting member to the outside of the tunnel. The

movable prongs are slightly shorter than the fixed prongs to allow the movable wire to swing past the fixed wire and thereby permit settings on either side. This clearance was usually no more than a few tenths of a millimeter. Distances were indicated on a linear scale below the tunnel by means of a pointer attached to the vertical shaft carrying the movable prongs. The height of the apparatus was such as to place the wires in the center of the tunnel when in use. The wires were of platinum 0.016 millimeter in diameter and about 5 millimeters long, care being taken to make the lengths of the two as nearly equal as possible. Soft solder was found to be very convenient and quite satisfactory for attaching the wires to the prongs.

The displacement of the movable wire by the swinging motion just described has the disadvantage that the wire moves in an arc of a circle rather than in a straight line and so suffers a downstream displacement as well as a lateral one. This defect increases in importance with the magnitude of the spacing; but, since neglecting the downstream displacement could not introduce an error greater than 2 percent in the measured scale of the turbulence for the greatest spacings encountered, no attempt was made to take it into account.

VARIATION OF CORRELATION WITH DISTANCE

With the apparatus placed at various distances back of the screens listed in table I, traverses were made by taking meter readings for various settings of the movable wire relative to and on either side of the fixed wire. The results obtained are illustrated in figure 5 by the plotted points and the solid curves. The positive and negative branches are the result of taking observations with the movable wire set first to one side and then to the other side of the fixed wire. Among the features to be noted are: first, the order of magnitude of the distance over which correlation exists and, second, the increase in this distance with increasing screen size.

The absence of points at the top of the curves indicates that it was never possible to observe the perfect correlation that must exist in the imaginary case of two coalescing wires. One reason for this difficulty is apparent when it is realized that the wires cannot be brought together without mutual interference. When the movable wire began to enter the wake of the fixed wire, a sharp reduction of correlation was observed. These data are not shown in the figure. Another cause of incomplete correlation near zero is the initial displacement necessary to allow the wires to pass one another. The effect of this displacement will be taken up in greater detail in part V. Another possible cause is a poor matching of the wires; but, as shown by the following example, this feature is not so important as might be supposed. If we reconsider equations (1), (2), and (4) with the response produced by u_1 differing from that produced by u_2 by a factor k, we obtain:

$$M_a=K\overline{(u_1k+u_2)^2}=K(k^2\overline{u_1^2}+\overline{u_2^2}+2k\overline{u_1u_2})$$

$$M_b=K\overline{(u_1k-u_2)^2}=K(k^2\overline{u_1^2}+\overline{u_2^2}-2k\overline{u_1u_2})$$

$$\frac{M_a-M_b}{M_a+M_b}=\frac{2k}{k^2+1}\,\frac{\overline{u_1u_2}}{\overline{u^2}}$$

where $\overline{u_1^2}=\overline{u_2^2}=\overline{u^2}$. If we suppose k to equal 0.8, then $\frac{2k}{k^2+1}=\frac{1.6}{1.64}=0.976$. In other words, if the two wires differed in length by 20 percent, the final result would be reduced by only 2.4 percent.

As was pointed out earlier, R' is not the correlation between the velocity fluctuations at two points in the stream, but is rather the correlation between the fluctuations over two wires—in this case, over wires 5 millimeters in length. Figure 5 shows that the correlation drops considerably in a distance of 5 millimeters; hence speed fluctuations at points, say at the center of each wire, must be different from those that are found for the average over the whole wire. Qualitatively at least it may be seen that the difference between the observed correlation and that existing between points will depend on the length of the wires and the rapidity with which correlation falls off with distance. In part IV, methods are developed for correcting all hot-wire results, whether of correlation or percentage turbulence, for this lack of complete correlation over the entire length of the wire or wires used. The R curves shown by the broken line in figure 5 were obtained by applying this correction to the R' curves. The R curves therefore represent the variation of correlation with distance between points and are consequently independent of wire length.

To compute R curves from the many observed R' curves, would have proved quite laborious; hence the procedure adopted was to obtain by graphical integration of the R' curves the observed scale of the turbulence L', defined as

$$L'=\int_0^\infty R'(y)\,dy$$

and then to correct these by dividing by the factor K_2, given in part IV, and so obtain the true scale of the turbulence L, defined as

$$L=\int_0^\infty R(y)\,dy$$

CHARACTERISTIC LENGTH OR SCALE OF TURBULENCE

In table II are given the values of L' and L expressed as fractions of the mesh size M of the screen that produced the turbulence. A comparison between $\frac{L'}{M}$ and $\frac{L}{M}$ will show the magnitude of the wire-length cor-

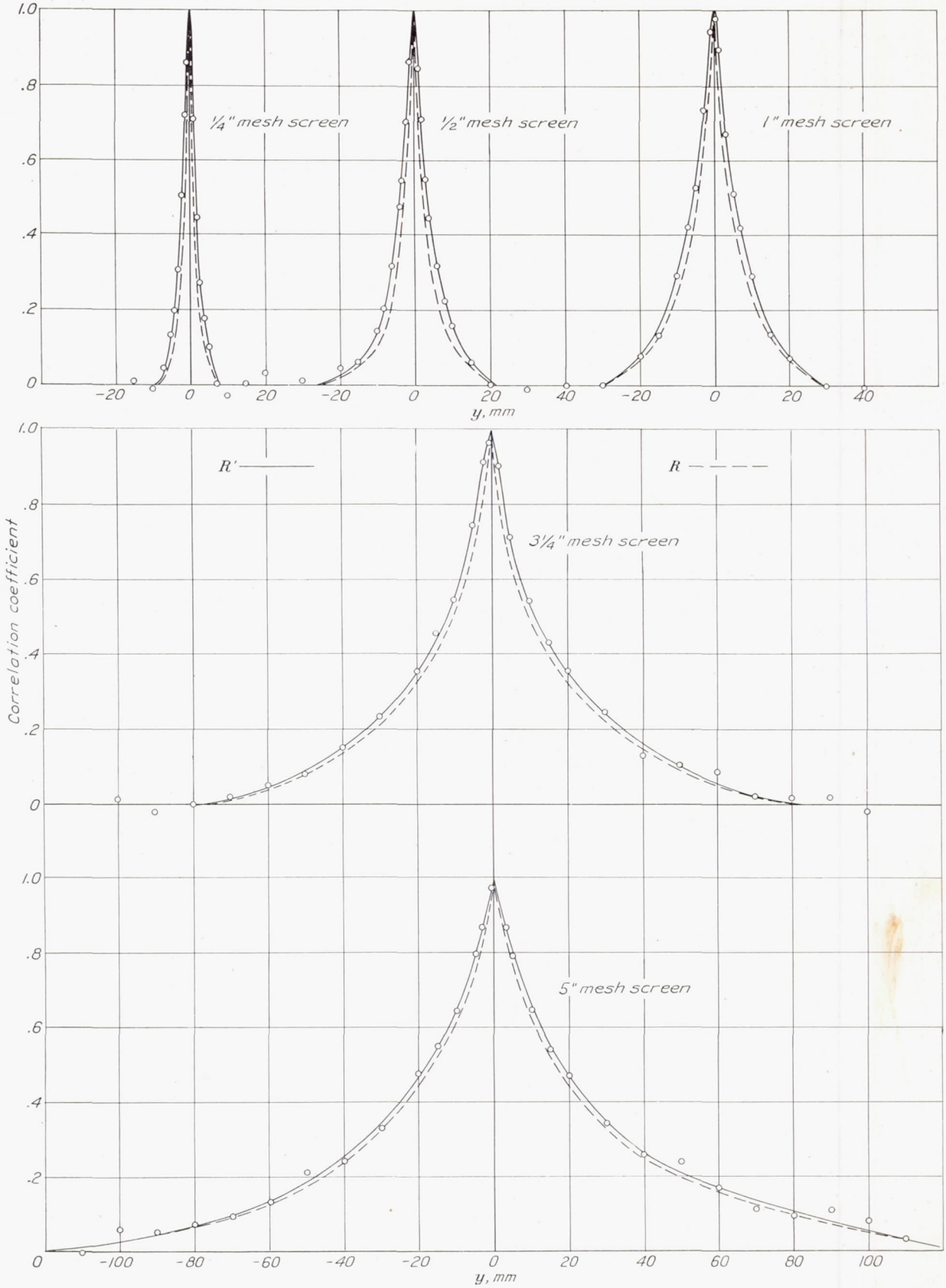

FIGURE 5.—Curves showing variation of correlation coefficient with the cross-stream separation of the hot wires. R' observed curves, R curves resulting when wire-length correction is applied. Observations taken 40 mesh lengths from screens. Wind speed 40 ft./sec.

rection. In order to put the results for the several screens on a comparable basis, distances downstream from the screens, as well as L' and L, have been expressed in terms of the mesh of the screens; that is, in terms of $\frac{x}{M}$, where x is distance downstream measured from the screen. It will be apparent that the scale of

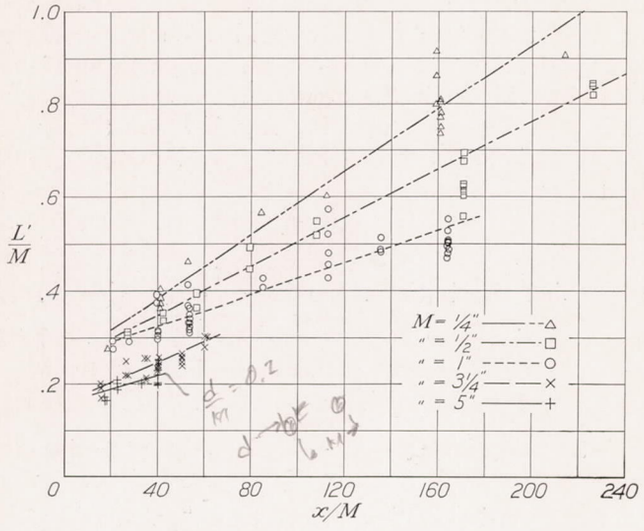

FIGURE 6.—Observed scale of turbulence at several distances from the screens.

$L'=\int_0^\infty R'(y)\,dy$, M=mesh of screen.

the turbulence produced by a given screen is not a constant quantity but increases with distance from the screen. With the exception of the dependence of the scale on the size of the screen and distance from the screen, L appeared to be unaffected by varying conditions of the stream. For example, no effect of air

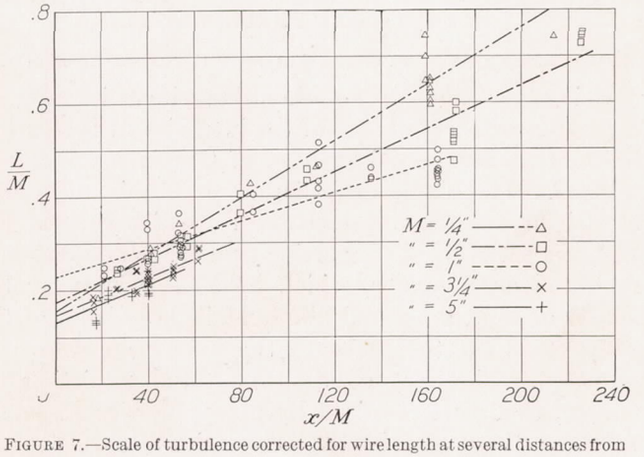

FIGURE 7.—Scale of turbulence corrected for wire length at several distances from the screens. $L=\int_0^\infty R(y)\,dy$, M=mesh of screen.

speed great enough to appear above the experimental variations could be found even though tests were made repeatedly to find an effect; nor did any variation with air temperature appear, even for such variation as from 12° C. to 30° C. Nearly all of the measurements given in the table were made at an air speed of 40 feet per second.

The important facts about L' and L are more clearly shown in figures 6 and 7 where $\frac{L'}{M}$, and $\frac{L}{M}$, respectively are plotted against $\frac{x}{M}$. It may be noted first that the increase with distance is quite marked, and second that the values of $\frac{L'}{M}$ show much more of a systematic change from screen to screen than do values of $\frac{L}{M}$. In fact, values of $\frac{L}{M}$ seem to be grouping close to a single curve. Systematic differences still exist, however, between the results for the several screens in figure 7 and show that the turbulent patterns are not exactly similar. This condition may be due to lack of similarity in the screens or to the residual turbulence produced by the honeycomb in the entrance of the tunnel. Table I and figure 2 show that the screens are similar in regard to major dimensions but different in details of construction. In view of these causes of departure from a single relation, separate curves were put through each set of points.

In figure 6, straight lines were arbitrarily drawn through the points without much consideration as to the appropriate type of curve. The curves of figure 7 were, however, drawn only after considerable study, since it was necessary to know the type of curve representing the relation or relations between $\frac{L}{M}$ and $\frac{x}{M}$ for future applications. Using the method of least squares, relations of the form

$$\frac{L}{M}=a_1+b_1\frac{x}{M}+c_1\left(\frac{x}{M}\right)^2$$

and

$$\frac{L}{M}=a+b\frac{x}{M}$$

were fitted to the data for each screen separately and to the data for all screens taken together. When the second-degree equation was tried, the coefficient c_1 came out positive for some screens and negative for others, a condition which led to the conclusion that the data could be represented more consistently by the simpler linear relation. Least-square straight lines have therefore been drawn through the points of figure 7. The equations of the separate lines, as well as of a single line fitted to all the data are listed in table III.

Both figures 6 and 7 show a scatter among the points which indicates either a change in the turbulent pattern from time to time or considerable experimental uncertainty. In the worst cases the maximum spread among repeated determinations of $\frac{L}{M}$ for the same screen and the same position reached 30 percent, and in such cases the average deviation from the mean was as great as 10 percent. It will be seen from the curves

that the scatter was less than this for many of the determinations. Extensive study was given to possible causes of these variations, after which it was concluded that the main cause lay in the uncertainty involved in determining the point where the correlation reached zero; that is, where the curves of figure 5 touch the y axis. This uncertainty could be traced to the variations in the meter readings caused by the longer period fluctuations. These variations tended to make the meter difficult to read, especially when the wires were far apart, and to mask the initial changes in the average meter reading accompanying the onset of correlation as the wires were brought together.

The linear law of increase in L should not be regarded as a universal one applying to turbulence regardless of source. Neither should it be regarded as strictly true for the turbulence produced by screens, since there can be little doubt that some residual turbulence from the honeycomb was present in all cases. The important fact here is that under a particular set of conditions the scale of the turbulence for an air stream is given by figure 7; and keeping these conditions the same, the figure may be used to indicate the scale in connection with the investigation of other properties and effects of turbulence, such as those given in subsequent parts of the report.

TAYLOR'S THEORY OF CORRELATION

In reference 8, G. I. Taylor gives the relation

$$R=1-\frac{y^2}{2!\overline{u^2}}\overline{\left(\frac{\partial u}{\partial y}\right)^2}+\frac{y^4}{4!\overline{u^2}}\overline{\left(\frac{\partial^2 u}{\partial y^2}\right)^2}-\cdots\cdot$$
$$(-1)^n\frac{y^{2n}}{(2n)!\overline{u^2}}\overline{\left(\frac{\partial^n u}{\partial y^n}\right)^2} \tag{5}$$

which was deduced from quite general considerations. The assumptions involved are, first, the physical one that $\overline{u^2}$ does not vary with y and, second, a mathematical one that it is possible to differentiate an averaged quantity. Both assumptions appear to be legitimate. From this relation it follows that R must be an even function of y. In reference 5, Taylor has extended his deductions as follows:

In the neighborhood of $y=0$, it is evident that a good approximation of the equation (5) is afforded by

$$R=1-\frac{y^2}{2!\overline{u^2}}\overline{\left(\frac{\partial u}{\partial y}\right)^2} \tag{6}$$

where the terms of y^4 and higher powers have been neglected. Equation (6) should then closely represent the region of the curve of R plotted against y near $y=0$. Solving equation (6) for $\overline{\left(\frac{\partial u}{\partial y}\right)^2}$, we get

$$\overline{\left(\frac{\partial u}{\partial y}\right)^2}=2\overline{u^2}\,Lt_{y\to 0}\left(\frac{1-R}{y^2}\right) \tag{7}$$

It is interesting to examine the curves of figure 5 in the light of the foregoing theory. The restriction imposed by equation (5) that R be an even function of y requires that the curves leave the axis $y=0$ with zero slope. This condition was never found in the observed R' curves, possibly because it was impossible to examine the top of the curves in detail due to their extreme narrowness. A slight rounding is apparent at the apex in all of the R' curves, but this has disappeared with the application of the wire-length correction and is not at all in evidence in the R curves. As seen from figure 21 in part IV, where the difference between the R' and R curves is small, the R curve may be closely represented by

$$R=e^{-\frac{y}{L}} \tag{8}$$

for which the initial slope is $-\frac{1}{L}$. In view of the uncertainties near $R=1$, however, it is quite possible that a sharp change in the slope begins near the origin of y to allow the initial slope of zero as required by equation (5) instead of $-\frac{1}{L}$ given by equation (8).

If R in equation (7) is replaced by $e^{-\frac{y}{L}}$, it may be seen by expansion of the exponential and passing to the limit $y=0$ that $\overline{\left(\frac{\partial u}{\partial y}\right)^2}$ becomes infinite. This condition is obviously impossible since, as will be seen by equation (13), the rate of dissipation of energy in the turbulent motions must then be infinite. It must be concluded therefore that equation (8), although a good approximation on the average, is not correct near $R=1$.

II—MEASUREMENTS OF INTENSITY AND RATE OF DECAY OF TURBULENCE

MEASUREMENTS OF THE INTENSITY BY THE HOT-WIRE METHOD

Using the hot-wire method described in part I, measurements were made of the intensity of the turbulence at various positions back of the screens listed in table I. The single hot wire used in this work was electrically welded to steel needles which formed the tips of a set of fixed supporting prongs.[3] These prongs mounted on a holder, which held the wire near the center of the tunnel and about 18 inches ahead of the supports, took the place of the apparatus shown in figure 4. The rest of the apparatus—omitting, of course, that part required by a second wire—was the same as that used in the correlation measurements. The wire was of platinum 0.016 millimeter in diameter and was about 5 millimeters long for the more recent set of measurements.

In earlier work, before the importance of the wire-length correction was recognized, a wire of about 1

[3] Electrically welding the wire to the prongs is generally found to be superior to soft soldering in the measurement of percentage turbulence because of the necessity of maintaining the calibration of the wire over long periods of time. This requirement was not so stringent in the correlation work since there the properties of the wire and its junctions needed to remain constant only during the time of a traverse.

centimeter length was usually used to gain greater sensitivity than was afforded by a shorter wire. The most recent of such measurements taken with a wire length of 8.4 millimeters, which at the same time apply to the turbulence produced by the screens listed in table I, are given in references 9 and 10. For purposes of comparison, these results are given here in table IV and in figures 8 and 9, along with the more recent results ob-

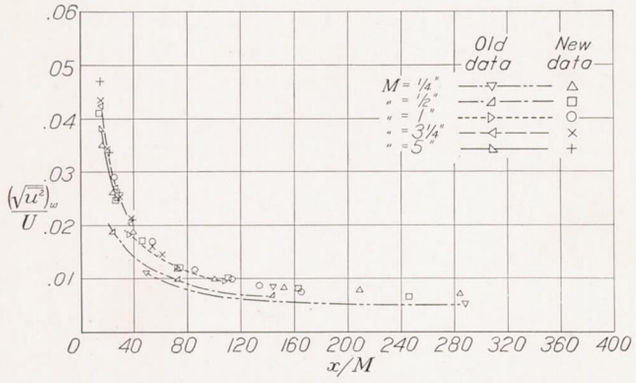

FIGURE 8.—Intensity of turbulence obtained with wires of different length at several distances from the screens. Old data—wire length 8.4 mm. New data—wire length 4.7 mm. (Wire-length correction not applied.) M=mesh of screens.

tained with a wire of length 4.7 millimeters. Both sets of results are plotted with x/M as abscissa in figure 8, without being corrected for the effect of wire length, and in figure 9 with the wire-length correction applied. The uncorrected values are denoted by the subscript w.

It may be noted in figure 8 that the results obtained with the 8.4-millimeter wire show a systematic increase for increasing mesh size for all screens except the 3¼- and 5-inch mesh. The results for the 4.7-millimeter

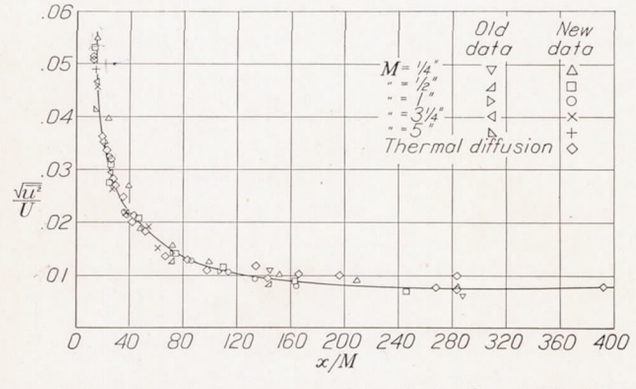

FIGURE 9.—Intensity of turbulence corrected for wire length at several distances from the screens. Old data—wire length 8.4 mm. New data—wire length 4.7 mm. M=mesh of screens.

wire show much less of this tendency and no attempt has been made to draw separate curves through the points. They fall distinctly above the value for the 1-, ½-, and ¼-inch screens obtained with the longer wire but are in fair agreement with the long wire results for the 3¼- and 5-inch mesh screens.

Before the results with the shorter wire were available, the occurrence of the separate curves for the several screens was believed to be due in part at least to an effect of wire length in relation to the scale of the turbulence; but there still remained the possibility of a lack of similarity in the turbulent flow pattern, caused perhaps by some departure from geometrical similarity in the screens themselves. When the results for the shorter wires were obtained, it became certain that the effect of wire length was largely responsible for the systematic differences. By that time the reason for such an effect was understood and the method of correction given in part IV was available. Figure 9 shows the result of applying the corrections. The systematic differences have been greatly reduced and the values for the long and short wires have been brought into agreement. The magnitude of the correction applied to the individual values may be judged from table IV, where both the corrected and uncorrected values are given.

The hot-wire measurements at any given point were always made at a number of wind speeds ranging usually from 20 to 70 feet per second. Throughout this range $\sqrt{\frac{\overline{u^2}}{U}}$ was found to be independent of the speed.

MEASUREMENTS OF THE INTENSITY BY THE THERMAL DIFFUSION METHOD

Figure 9 also shows good agreement between the corrected values of the turbulence obtained by the hot-wire method and those obtained by the method of thermal diffusion. The latter is an independent method of measuring the intensity of the turbulence, the technique of which is described in reference 9. The measurements from which the values given in figure 9 were calculated are also given in this reference for the screens listed in table I. The points for the several screens are not given separate designation since no systematic differences from screen to screen appeared.

Briefly the method of thermal diffusion consists of determining the width of the heated wake at a fixed distance back of a rather long but fine heated wire in the air stream by traversing the wake with a small thermocouple. In the measurements of reference 9 the width of the wake at half the temperature rise at the center of the wake, obtained from the curve of temperature distribution across the wake, was used as a measure of the width. The apparatus was so arranged that the angle subtended at the heating wire for different positions of the thermocouple was obtained; hence the results are given in terms of the angle subtended by the width of the wake at half maximum temperature. After the angle had been corrected for the spreading of the wake caused by the thermal conductivity of the air, it was found that the remaining angle, denoted by α_{turb}, was directly proportional to the turbulence in the stream and independent of the scale. For the conditions obtaining in the experiment it is possible to apply the theory of diffusion by continuous movements given by Taylor in reference 8 to calculate the intensity

of the turbulence from α_{turb} directly.[4] The equations leading to the calculation are given in reference 5 in a form directly applicable to the results of reference 9. These original references should be consulted for details; it suffices to state here that the relation connecting α_{turb} and the intensity of the turbulence is

$$\alpha_{turb}\ (\text{degrees}) = 134.9\frac{\sqrt{\overline{v^2}}}{U}$$

where $\sqrt{\overline{v^2}}$ is the root-mean-square of the cross-stream component of the fluctuation velocity and U is the average speed of the stream.

It will be observed that $\frac{\sqrt{\overline{u^2}}}{U}$ is obtained by the hot-wire method, whereas $\frac{\sqrt{\overline{v^2}}}{U}$ is obtained from thermal diffusion. The fact that $\frac{\sqrt{\overline{u^2}}}{U}$ agrees well with $\frac{\sqrt{\overline{v^2}}}{U}$ in figure 9 indicates that the turbulence must be closely isotropic; that is, that the cross-stream fluctuations are on the average the same as those along the stream. The agreement of the values obtained by these two independent methods also furnishes good evidence that the method of correcting the hot-wire results for wire length is reliable.

No effect of wind speed on the value of α_{turb} could be found throughout the range of speeds investigated, which ranged from 8 to 55 feet per second. The thermal diffusion method then offers additional evidence that the intensity of the turbulence does not vary with wind speed.

THEORY OF DECAY OF TURBULENCE

The usual concept of turbulence is that small fluid masses moving with velocities relative to one another give rise to the observed velocity fluctuations whose root-mean-square value is used as a measure of the intensity of the turbulence. The average distance over which the fluctuations may be regarded as completely correlated will serve as a measure of the average linear dimension of the fluid masses. The average velocity of the masses with respect to the mean velocity may then be identified[5] with $\sqrt{\overline{u^2}}$, the intensity as given by the hot-wire anemometer; and the average linear dimension may be identified with L, the scale as obtained from the area under the correlation curves.

In order to obtain the law of decay of turbulent motions, it is necessary to know the equation of motion of the fluid masses. In the choice of this equation we are guided by the fact that the solution must yield results in accordance with experiment, which are that the rate of decay is a function of $\frac{x}{M}$ and that $\frac{\sqrt{\overline{u^2}}}{U}$ is independent of the average speed U.

Let us assume that the force resisting the motion of the fluid mass is proportional to the product of density by cross-sectional area by the square of its speed relative to the mean flow. If m is the mass of fluid moving with velocity $\sqrt{\overline{u^2}}$, C_1 is the resistance coefficient, and t is the time, the equation of motion is

$$m\frac{d\sqrt{\overline{u^2}}}{dt} + C_1\rho L^2\overline{u^2} = 0 \tag{9}$$

Setting m proportional to ρL^3

$$L\frac{d\sqrt{\overline{u^2}}}{dt} + C_2\overline{u^2} = 0$$

Integrating

$$\frac{1}{(\sqrt{\overline{u^2}})_0} - \frac{1}{\sqrt{\overline{u^2}}} = -C_2\int_0^t \frac{dt}{L}$$

where $(\sqrt{\overline{u^2}})_0$ is the value of $\sqrt{\overline{u^2}}$ at $t=0$. Taking the origin of the turbulence at the screen and x as the distance downstream from the screen, we may set $t=\frac{x}{U}$ where U is the average speed of the stream. When this substitution is made the law of decay becomes

$$\frac{U}{(\sqrt{\overline{u^2}})_0} - \frac{U}{\sqrt{\overline{u^2}}} = -C_2\int_0^x \frac{dx}{L} \tag{10}$$

This equation satisfies the requirement that $\frac{\sqrt{\overline{u^2}}}{U}$ is independent of U if $\frac{(\sqrt{\overline{u^2}})_0}{U}$ is independent of U. We may infer that this last condition is true from the observation that the resistance of any given screen varies approximately as the square of the wind speed and hence that the flow in the immediate vicinity of the screen remains similar at different speeds.

It may be shown that no other resistance law in which the resistance is expressed as a function of the velocity will lead to a law of decay giving $\frac{\sqrt{\overline{u^2}}}{U}$ independent of U.

Taylor derives the law of decay expressed by equation (10) in a somewhat different way. He assumes (reference 5) from the phenomena of turbulent flow in pipes that the average rate of dissipation of energy per unit volume is given by the expression

$$\overline{W} = \frac{C_3\rho(\sqrt{\overline{u^2}})^3}{L} \tag{11}$$

The dissipative stresses within the medium, which act in opposition to the motion of elementary turbulent currents in the manner expressed by equation (9), arise from the action of viscosity in regions where

[4] This calculation is rigorous only when the fluctuation velocity of a particle at the heating wire and that of the same particle after the interval of time required for the particle to reach the thermocouple are perfectly correlated. The distance of 2 inches between the heating wire and the thermocouple, which existed when α_{turb} was measured, was small enough and the time interval consequently short enough to prevent any detectable departure from perfect correlation for all the screens. In fact, no departure from perfect correlation could be detected even at 6 inches. Unfortunately, reference 8 was not discovered before the publication of reference 9, and as a result this important calculation was not included.

[5] Actually, $\sqrt{\overline{u^2}}$ is the root-mean-square of the x component of the velocity fluctuations. In the equations to follow, the total velocity of the fluid masses should be used; but since $\overline{u^2}=\overline{v^2}=\overline{w^2}$, the total velocity will differ from the x component only by a numerical factor. This factor will be absorbed along with other factors of proportionality in the constants C_1, C_2, C_3, etc.

velocity gradients exist. In terms of the velocity gradients and the viscosity the rate of dissipation may be expressed by

$$\overline{W}=\mu\left\{2\overline{\left(\frac{\partial u}{\partial x}\right)^2}+2\overline{\left(\frac{\partial v}{\partial y}\right)^2}+2\overline{\left(\frac{\partial w}{\partial z}\right)^2}+\overline{\left(\frac{\partial w}{\partial y}+\frac{\partial v}{\partial z}\right)^2}+\overline{\left(\frac{\partial u}{\partial z}+\frac{\partial w}{\partial x}\right)^2}+\overline{\left(\frac{\partial v}{\partial x}+\frac{\partial u}{\partial y}\right)^2}\right\} \tag{12}$$

where μ is the coefficient of viscosity and u, v, and w are the fluctuation velocities in the x, y, and z directions, respectively. For isotropic turbulence Taylor, in reference 5, has reduced equation (12) to the form

$$\overline{W}=7.5\mu\overline{\left(\frac{\partial u}{\partial y}\right)^2} \tag{13}$$

Two expressions therefore exist for the mean rate of dissipation of turbulent energy: Equation (11) in terms of the fluctuation velocities and the scale, and equation (13) in terms of the velocity gradients due to the fluctuations. As has been pointed out in part I, $\overline{\left(\frac{\partial u}{\partial y}\right)^2}$ determines the shape of the top of the correlation curves near the value of $R=1$, and in principle at least, the dissipation could be determined from equation (13) with the aid of the correlation curves. As has been seen, the correlation curves under the conditions of the present experiments are too narrow at the top to permit the accurate determination of the dissipation in this way.

The turbulent energy content per unit volume of the fluid is $\frac{1}{2}\rho(\overline{u^2}+\overline{v^2}+\overline{w^2})$ or since $\overline{u^2}=\overline{v^2}=\overline{w^2}$, is $\frac{3}{2}\rho\overline{u^2}$. The rate of change of this energy, or the rate of dissipation is therefore

$$\overline{W}=-\frac{3}{2}\rho\frac{d(\overline{u^2})}{dt}=-\frac{3}{2}\rho U\frac{d(\overline{u^2})}{dx} \tag{14}$$

where U is the average speed of the stream and x is distance along the stream. Equating the two expressions for $\overline{W}$ given in equations (11) and (14) and simplifying, we get

$$-\frac{Ud\left(\sqrt{\overline{u^2}}\right)}{\left(\sqrt{\overline{u^2}}\right)^2}=C_4\frac{dx}{L} \tag{15}$$

which is equivalent to equation (10).

Equation (15) may be put in the form

$$-\frac{Ud\left(\sqrt{\overline{u^2}}\right)}{\left(\sqrt{\overline{u^2}}\right)^2}=C_4\frac{d\left(\frac{x}{M}\right)}{\frac{L}{M}} \tag{16}$$

in which $\frac{L}{M}$ may be replaced by $a+b\frac{x}{M}$, given in part I. Substituting and integrating, we get

$$\frac{U}{\sqrt{\overline{u^2}}}-\frac{U}{\left(\sqrt{\overline{u^2}}\right)_0}=\frac{C_5}{b}\log_e\left(1+\frac{b}{a}\frac{x}{M}\right)$$

or changing to $\log_{10}$

$$\frac{U}{\sqrt{\overline{u^2}}}-\frac{U}{\left(\sqrt{\overline{u^2}}\right)_0}=\frac{C_6}{b}\log_{10}\left(1+\frac{b}{a}\frac{x}{M}\right) \tag{17}$$

where $\left(\sqrt{\overline{u^2}}\right)_0$ is the value of $\sqrt{\overline{u^2}}$ at $\frac{x}{M}=0$. The same result would have been obtained from equation (10) had the relation between $\frac{L}{M}$ and $\frac{x}{M}$ been substituted there.

In figure 10 $\frac{U}{\sqrt{\overline{u^2}}}$ has been plotted against $\frac{1}{b}\log_{10}\left(1+\frac{b}{a}\frac{x}{M}\right)$, where a and b have been given the separate

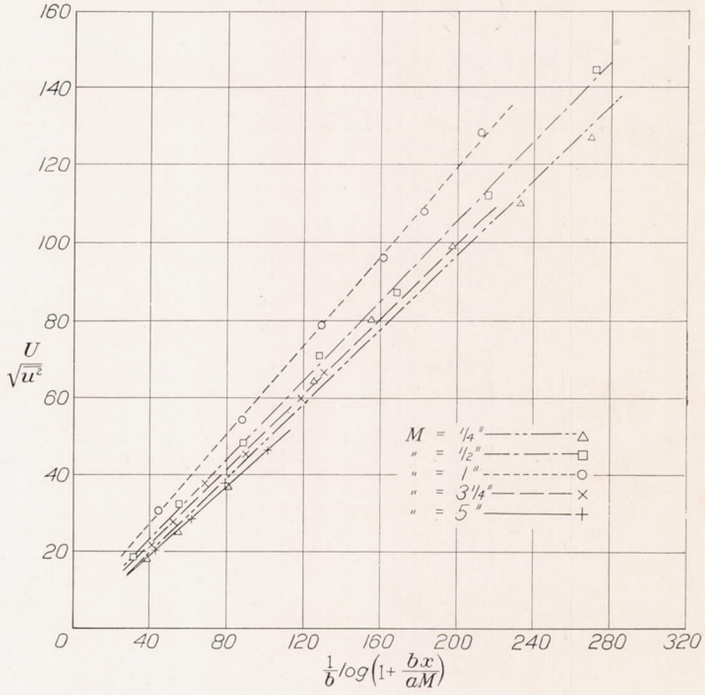

FIGURE 10.—Test of law of decay, $\frac{U}{\sqrt{\overline{u^2}}}-\left(\frac{U}{\sqrt{\overline{u^2}}}\right)_0=\frac{C_6}{b}\log_{10}\left(1+\frac{b}{a}\frac{x}{M}\right)$. Values of a and b are given in table III.

values for the several screens from table III. The plot has been made using only the data for the 4.7-millimeter wire, which is believed to be less subject to error in the wire-length correction than the data for the longer wire. The points are seen to lie along straight lines as well as may be expected from the experimental precision. The separate curves for each screen are due to some extent to the systematic differences from screen to screen in figure 9, not clearly shown by that type of plot, but are to a greater extent due to the separate curves used to represent the relation between $\frac{L}{M}$ and $\frac{x}{M}$ in figure 7; that is, to the different values of a and b. The evidence afforded by figure 10 that equation (17) is of the proper form to represent the decay is to show further that the three experimental facts:

1. $\frac{\sqrt{\overline{u^2}}}{U}$ independent of U

2. A decay of $\frac{\sqrt{\overline{u^2}}}{U}$ given by figure 9

3. An increase of $\frac{L}{M}$ given by figure 7

are all consistent with one another. Having given any two of these conditions, the third must follow.

By least square fitting of the straight lines in figure 10 to the data, the constants $\frac{U}{(\sqrt{\overline{u^2}})_0}$ and C_6 of equation (17) have been evaluated and tabulated in table V. The value of $\frac{U}{(\sqrt{\overline{u^2}})_0}$ is seen to vary considerably from screen to screen, which may be partly due to differences in the geometrical shapes of the screens but more probably to errors involved in the curve fitting. On the other hand, the coefficient C_6, which is closely analogous to a resistance coefficient of the fluid masses, is nearly constant.

To return to a more simple type of representation, we may consider figure 11, where $\frac{U}{\sqrt{\overline{u^2}}}$ has been plotted against $\frac{x}{M}$ for the several screens, along with the theoretical curves given by equation (17) with the constants listed in table V. The new data with the shorter wire from which the constants were evaluated must, of course, fit the curves. The old data obtained with the longer wire and the thermal diffusion data are added to show that they too are not inconsistent with the theory.

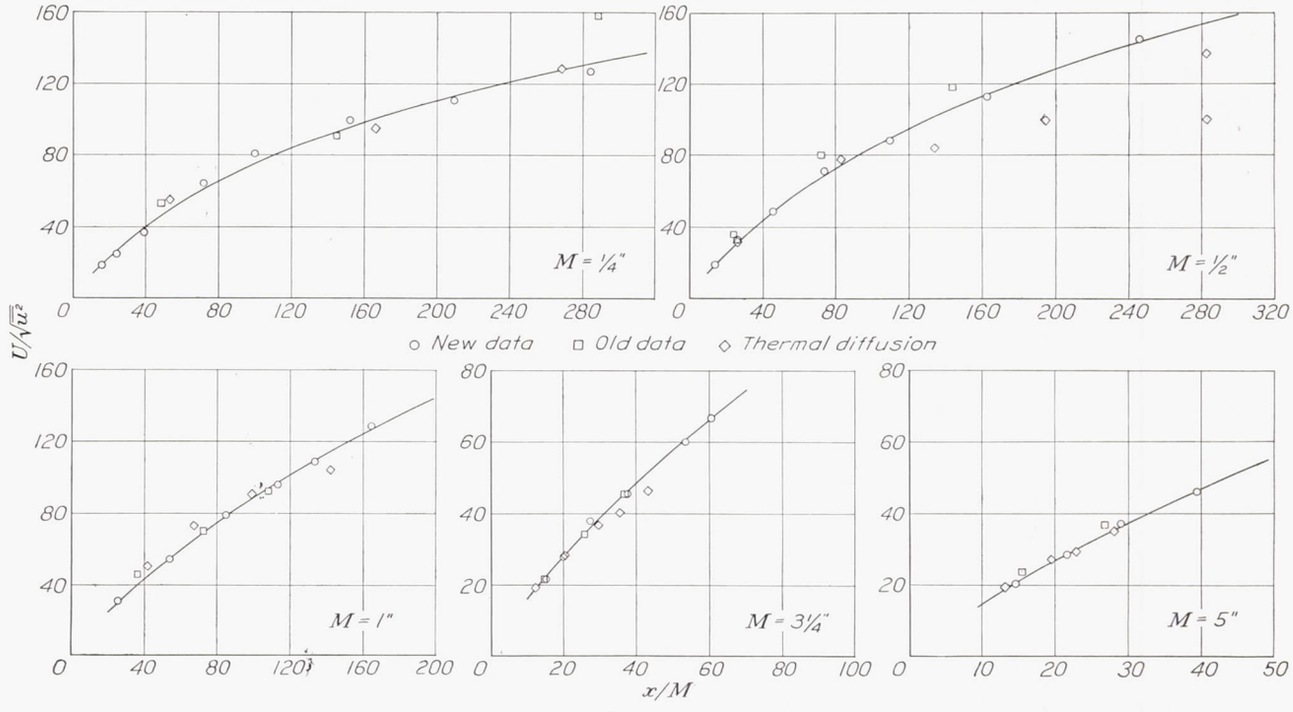

FIGURE 11.—Theoretical decay curves.

III—THE CRITICAL REYNOLDS NUMBER OF SPHERES

The use of a sphere as an indicator of turbulence in wind tunnels was originally proposed by Prandtl (reference 11). If one measures the drag force F on a sphere of diameter D in an air stream of speed U, the air being of density ρ, and viscosity μ, and plots the drag coefficient $C_D = \frac{F}{\frac{\pi}{4}D^2\frac{1}{2}\rho U^2}$ against the Reynolds Number $UD\frac{\rho}{\mu}$, it will be found that at low Reynolds Numbers C_D is approximately constant and equal to about 0.5. At Reynolds Numbers within a range of values dependent on the turbulence of the air stream C_D decreases rapidly to values in the neighborhood of 0.1. Prandtl suggested that "observation of such resistance curves for spheres gives a means of comparing the air streams of different laboratories, with respect to their lesser or greater turbulence." The decrease occurs at higher Reynolds Numbers in streams of lower turbulence.

When a technique had been developed for measuring the intensity of the speed fluctuations by means of the hot-wire anemometer and associated equipment, one of the authors with A. M. Kuethe attempted with some success to calibrate the sphere as a device for measuring the intensity of the turbulence (reference 1). To make the sphere results quantitatively definite, we proposed to define the critical Reynolds Number of a sphere as

the value of the Reynolds Number at which the drag coefficient of the sphere is 0.3.[6] This proposal has been rather generally adopted.

As more data were accumulated in wind tunnels with different honeycomb arrangements (references 2 and 3), the calibration of the sphere in terms of the intensity of the turbulence became more and more unsatisfactory. Millikan and Klein noted that the critical Reynolds Number depended on the diameter of the sphere. It became apparent that a more comprehensive study was needed.

Such a study has been carried out with the cooperation of the National Advisory Committee for Aeronautics. The general plan and the guiding principles have already been stated in the Introduction to this paper. The preceding sections give the methods by which the turbulence was varied, that is, by the use of a series of geometrically similar screens of square mesh. Measurements could be made at various distances from the screens. Data as to the intensity and scale of the turbulence at various distances are given in the preceding sections. The present section describes the measurements of the critical Reynolds Number of spheres and its variation with the intensity and scale of the turbulence.

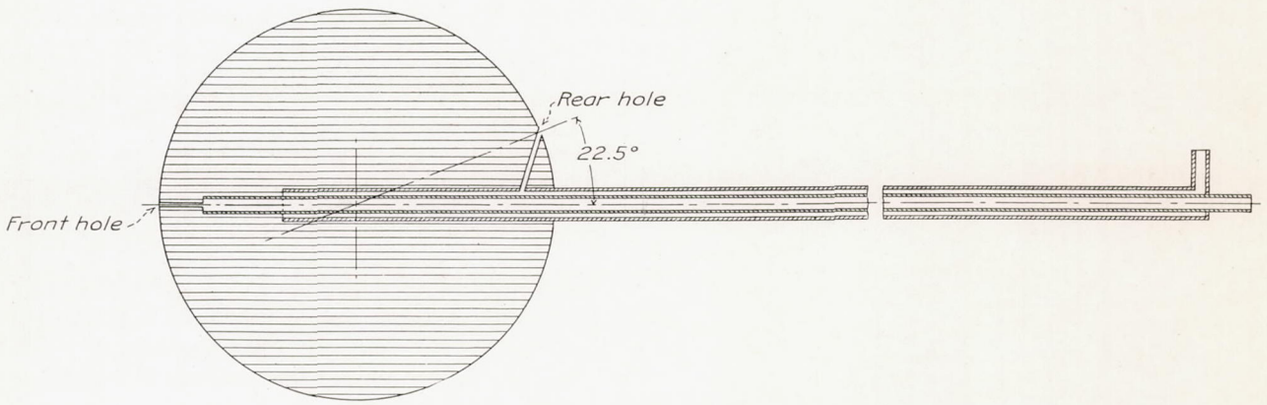

FIGURE 12.—The pressure sphere.

THE PRESSURE SPHERE

The measurement of the resistance of a sphere in wind tunnels of varying size is somewhat inconvenient. The accurate determination of the forces on the supports is time-consuming, and the fact that the balances in normal use are of greatly varying sensitivity in large and small wind tunnels necessitates the construction of a special balance of suitable sensitivity. To simplify the procedure we began in November 1933 the use of a "pressure-sphere" (references 12 and 13). The pressure-sphere is shown diagrammatically in figure 12. It consists of a smooth sphere [7] mounted on a tubular tail spindle. Within the tubular spindle is an inner concentric tube that connects to an impact hole diametrically opposite the spindle. In the hemisphere containing the spindle at an azimuth angle of 157½° from the impact hole, one or more holes are drilled to make connection to the annular space between the tubular spindle and the inner concentric tube. Suitable connecting nipples are provided at the end of the tail spindle.

The differential pressure between the impact hole and the wake can be measured by mounting the pressure-sphere rigidly with the tail spindle parallel to the direction of flow and connecting the nipples to the two sides of a manometer. The downstream holes were not located on the spindle or at the junction of sphere and spindle because we wished to avoid any necessity for controlling the exact geometrical form of the tail spindle.

The results are expressed in terms of a pressure coefficient obtained by dividing the differential pressure given by the pressure-sphere by the velocity pressure. For small Reynolds Numbers the pressure coefficient is approximately 1.4 and for high Reynolds Numbers about 0.9, the rapid decrease from one value to the other occurring at a Reynolds Number dependent on the turbulence of the air stream.

Mr. Robert C. Platt, of the Committee's staff at Langley Field, kindly undertook the comparison of the pressure-sphere results with force measurements for spheres of several sizes. He reported that a value of the pressure coefficient of 1.22 was approximately equivalent to a drag coefficient of 0.3. Hence it was decided to define the critical Reynolds Number of the pressure sphere as the Reynolds Number at which the pressure coefficient is 1.22. It is recognized that the equivalence is not an exact one. The detailed results obtained by Mr. Platt are described in reference 14.

A great advantage of the pressure sphere is the ease with which measurements may be made in flight or on a traveling carriage. Mr. Platt describes measurements of both types, which yield a value of the critical Reynolds Number in turbulence-free air of 385,000.

The pressure-sphere method was independently developed by S. Hoerner (reference 15) at the Deutsche

[6] We did not know at the time that Prandtl had suggested the use of the value 0.36.

[7] We have generally used standard bowling balls, diameter 5 inches or 8.55 inches. The departure of these balls from a spherical form is very small.

Versuchsanstalt für Luftfahrt, with some difference in detail. The rear holes were located in the tail spindle at its junction with the sphere. Pressures are referred to the static pressure of the air stream and hence the DVL pressure coefficients are equal to 1 minus our pressure coefficients. Hoerner used as critical Reynolds Number that for which the pressure at the rear holes was equal to the static pressure, corresponding to a pressure coefficient of 1.00 on our convention. Hence his values of critical Reynolds Number are somewhat higher than ours.

Hoerner also studied the relation between drag coefficient and pressure coefficient. His results on a single sphere in relatively smooth flow indicate that a pressure coefficient of 1.18 on our convention corresponds to a drag coefficient of 0.3, in fair agreement with the value of 1.22 obtained from the more extended measurements of Platt. It must be emphasized, however, that the relations between the values of the critical Reynolds Number as determined by drag measurements and by pressure measurements with different locations of the pressure openings are only approximate, and sufficient work has not been done to determine the influence of turbulence, sphere diameter, and exact location of the rear holes.

MEASUREMENTS WITH SPHERES

Some preliminary studies were made of the reproducibility of the results obtained with several supposedly identical pressure spheres. Three commercial 5-inch bowling balls were used to determine the critical Reynolds Number corresponding to the turbulence in the 3-foot wind tunnel of the National Bureau of Standards. The values obtained were 273,000, 276,000, and 272,000, which agree very well.

The extended series of measurements in the 4½-foot tunnel behind the several screens were made with two spheres, one 5 inches and the other 8.55 inches in diameter. The working distances could not exceed about 15 feet because of the limited length of the working section. In order to avoid large variations in mean speed, the closest distance had to be 15-mesh lengths or greater. Since the spheres are of finite size, extending over a distance of many mesh lengths for the smaller screens, the closest distance was further limited to avoid large changes of turbulence over the sphere. In no case was the closest distance less than 1 foot. The actual working distances, selected somewhat arbitrarily, were 1, 3, and 6 feet for the ¼- and ½-inch screens; 3, 6, and 9 feet for the 1-inch screen; 4, 7, and 10 feet for the 3¼-inch screen; 6 feet 5 inches and 11 feet 2 inches for the 5-inch screen.

The data obtained for the 1-inch screen are plotted in figure 13 for the 5-inch sphere and in figure 14 for the 8.55-inch sphere. The values of the critical Reynolds Number corresponding to the several distances were read from these and similar curves, the critical Reynolds Number being defined as previously explained as the Reynolds Number for which the pressure coefficient is 1.22. The results are given in table VI.

It will be noted that the curves of figures 13 and 14 show abrupt changes of slope at pressure coefficients of 1.1 to 1.15. After some investigation it was discovered that the use of four symmetrically located rear holes instead of a single hole gave curves without breaks, and hence that the breaks were probably due to local asymmetry in the flow about the sphere. Figure 15 shows curves obtained under the same conditions as the curves in figure 14 except that a sphere with four rear holes was used. The values of the critical Reynolds Numbers are unchanged and the breaks are absent.

In order to obtain some idea of the effect of the small departures from a uniform speed distribution, traverses were made with the sphere behind the 5-inch screen that showed the greatest departures. At a distance of 6.4 feet from the screen, the critical Reynolds Number was 107,000 and 109,000 in two runs at the center; 107,000, 2 inches below the center; 108,000, 4 inches below the center; and 109,000, 2 inches above the center. At a distance of 11.2 feet, values of 145,000 and 148,000 were obtained at two positions.

Table VI gives a summary of the pertinent data on the critical Reynolds Number. The values of $\frac{\sqrt{\overline{u^2}}}{U}$ are taken from the least-square lines of figure 10, and the values of L from the least-square lines of figure 7. Figures 16 and 17 show the relation between critical Reynolds Number and $\frac{\sqrt{\overline{u^2}}}{U}$ for the several screens as obtained with the 5 and 8.55 inch spheres, respectively. The points obtained at a distance of 1 foot (encircled in plotting) are not in good agreement with the other observations and the curves have not been extended through them. Evidently 1 foot is too close a working distance for spheres of this size. The observations show a systematic variation from screen to screen and a systematic variation with the diameter of the sphere. The larger the screen mesh, the greater the intensity required to give a specified critical Reynolds Number. The larger the diameter, the smaller the intensity required.

G. I. Taylor suggested in correspondence that the critical Reynolds Number should be a function of the quantity $\frac{\sqrt{\overline{u^2}}}{U}\left(\frac{D}{L}\right)^{\frac{1}{5}}$, where L is the scale of the turbulence. The data plotted in terms of this quantity are shown in figure 18. Except for the measurements made at a distance of 1 foot, the observations for both spheres and all screens lie remarkably well on a single curve, certainly within the observational errors.

The details of the reasoning that led Taylor to this suggestion have been published in reference 16. It may be stated in general terms that the foregoing combination of intensity and scale of turbulence occurs in the expression for the root-mean-square pressure gradient

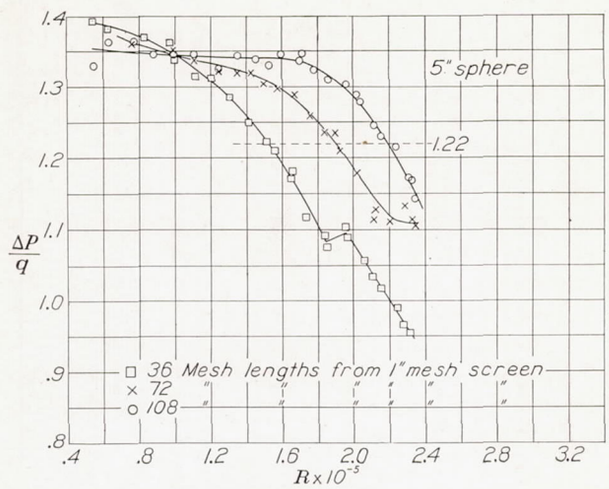

FIGURE 13.—Pressure coefficients for 5-inch sphere behind 1-inch screen.

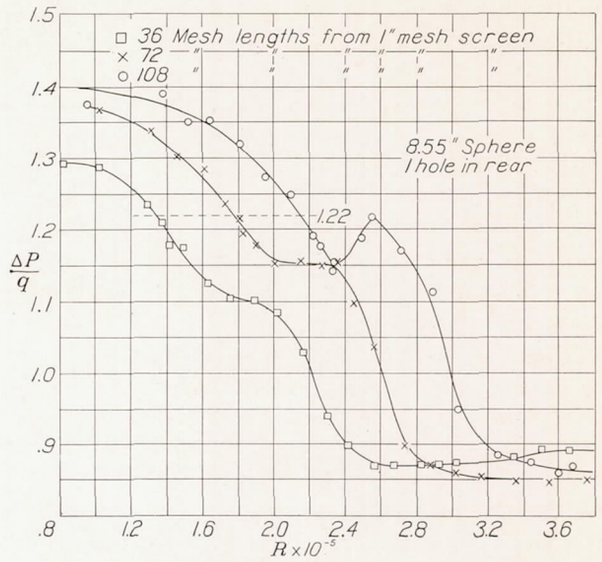

FIGURE 14.—Pressure coefficients for 8.55-inch sphere behind 1-inch screen.

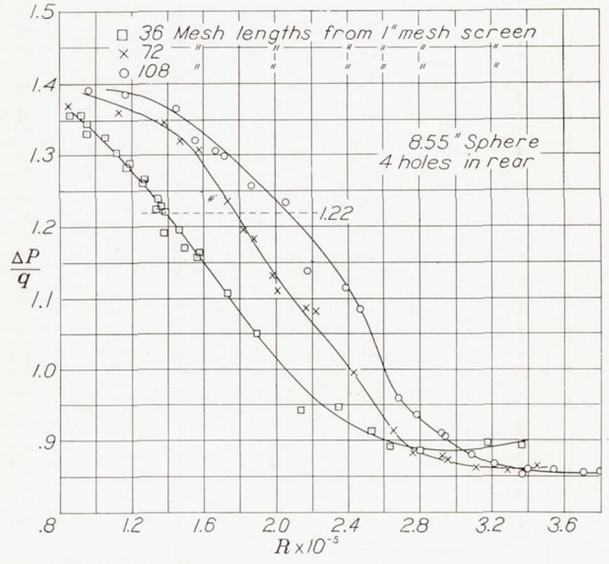

FIGURE 15.—Pressure coefficients for 8.55-inch sphere with four rear holes behind 1-inch screen.

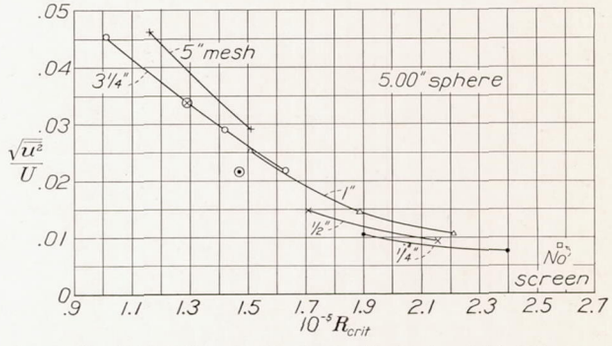

FIGURE 16.—Critical Reynolds Number for 5-inch sphere behind all screens.

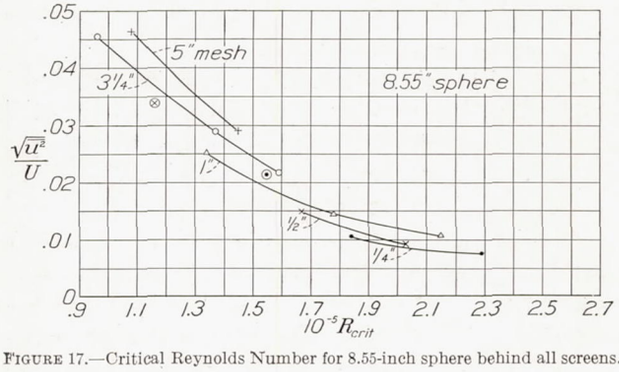

FIGURE 17.—Critical Reynolds Number for 8.55-inch sphere behind all screens.

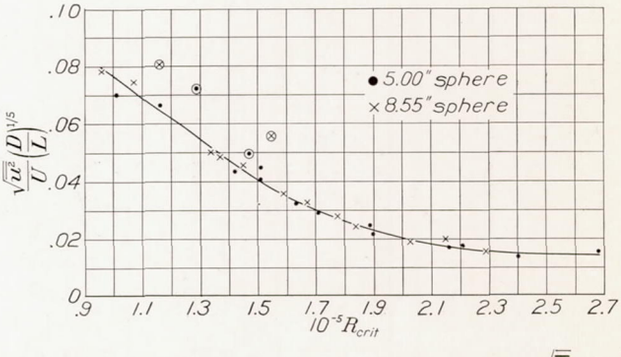

FIGURE 18.—Critical Reynolds Number of spheres as a function of $\frac{\sqrt{\overline{u^2}}}{U}\left(\frac{D}{L}\right)^{1/5}$.

in the turbulent flow, and that the effect of turbulence is assumed to be that of the pressure gradient on transition.

The wind-tunnel equipment available at the National Bureau of Standards unfortunately does not permit the extension of the curve in figure 18 to a critical Reynolds Number exceeding 270,000. In most of the more recently constructed wind tunnels, values exceeding this value are found. In the large tunnels, the large scale of the turbulence contributes to the high value but, in addition, the intensity is of the order of 0.7 percent or less. The accurate measurement of these small fluctuations is an experimental problem of very considerable difficulty.

DETERMINATION OF AVERAGE VELOCITY PRESSURE

In the production of artificial turbulence in wind tunnels for the purpose of studying the aerodynamic effects of turbulence, it is desired to vary the magnitude of the rapid fluctuations without introducing departures from a uniform distribution in space. Ower and Warden (reference 17) concluded that wire or cord networks were unsuitable because of the introduction of variations in the mean speed produced by the "shadows" of the wires. This general conclusion is somewhat tempered in their detailed discussion by the recognition that the uniformity will depend on the distance from the network at which observations are made and that the uniformity may be satisfactory at distances of the order of 144 wire diameters or 24 mesh lengths. In view of this criticism of networks as sources of turbulence it seems desirable to review the studies that were made behind the screens used in the present series of measurements to determine the degree of uniformity of the mean speed and the average value of the velocity pressure for computing the pressure coefficients of the spheres.

A preliminary series of traverses was made for the purpose of determining the distance at which the pattern of the screen disappeared. For the ¼-, ½-, and 1-inch-mesh screens, a simple impact tube with outside diameter of ⅛ inch and inside diameter of 1/16 inch was used, the static side of the manometer being connected to the wall plate used as a source of reference pressure in the operation of the tunnel. For the larger screens, a standard pitot-static tube was used. Observations were taken at about 24 points along a line parallel to the horizontal wires of the screen and in a horizontal plane passing midway between two wires of the screen. The spacing was 1/16 inch, ⅛ inch, ¼ inch, ½ inch, and 1 inch for the ¼-, ½-, 1-, 3¼-, and 5-inch-mesh screens, respectively. Traverses were made at several distances from about 4 to 20 mesh lengths from the screen. For distances less than 12-mesh lengths, the pressure varied regularly with maxima and minima corresponding to the spacing of the wires of the screen. The curves resemble those shown in reference 17 and are therefore not reproduced in this paper. At distances greater than 12-mesh lengths, there was no regular pattern.

In order to give some idea of the magnitude of the variation, the maximum and mean deviations of the single observations from their arithmetic mean have been computed and are tabulated in table VII. Both quantities are very large close to the screen but rapidly decrease. For distances greater than 12-mesh lengths the gain in uniformity is comparatively small. Hence it was concluded that observations should not in any case be made at distances closer than 12-mesh lengths and, as a precautionary measure, the closest distance used was actually 15-mesh lengths. From table IV, it is seen that the maximum value of $\frac{\sqrt{\overline{u^2}}}{U}$ is accordingly limited to about 0.05.

At the distances for which sphere data had been or were to be obtained, a more extended traverse was made with a standard pitot-static tube. Observations were taken at 12 equidistant points along circles of radii 2, 5, 8, 12, and 18 inches from the tunnel axis, in some cases for three speeds. The maximum and mean deviations of the single observations from their arithmetic mean are also tabulated in table VII for these traverses.

It will be observed that the mean deviations approach different values for the different screens as the distance from the screen is increased: 2.2 percent for the 5-inch screen, about 2.0 percent for the 3¼-inch screen, about 0.5 percent for the 1-inch screen, about 1.0 percent for the ½-inch screen, and about 1.0 percent for the ¼-inch screen. It is probable that these differences reflect corresponding differences in the geometrical accuracy of the spacing of the wires of the screen. The uniformity obtained with the 1-, ½-, and ¼-inch screens is comparable with that obtained in the free stream, the mean deviation of the pressure from the average being 1.0 percent or less, corresponding to 0.5 percent or less in the speed.

The measurements described in this paper extended over a considerable period of time and it was not practicable to install a screen and complete all measurements before removing the screen, because of the necessity of making other tests. The procedure in most of the sphere tests was to determine the ratio of the velocity pressure at the axis of the tunnel to the reference wall plate pressure as a function of the speed; then at one value of the reference pressure to determine the speeds at six points on a circle of 2-inch radius. A faired curve through the points observed in the first run was adjusted as indicated by the ratio of the mean of the six values on the 2-inch circle and the value at the center to the value at the center. For all screens except the 3¼-inch screen, the value adopted did not differ from that given in table VI by as much as the mean deviation given in that table. For one installa-

tion of the 3¼-inch screen, the difference somewhat exceeded the mean deviation.

From a study of the results given later, an error of 1 percent in the determination of the mean velocity pressure produces an average change of $4{,}500 \pm 500$ in the value of the critical Reynolds Number. It is believed that the error in the values used did not in any case exceed the mean deviation given in table VII and was probably less than half that value, which represents the mean deviation over an area much larger than the sphere. The effect of the small departures from a constant speed (as contrasted with an error in the average speed) on the value of the critical Reynolds Number is not known but is probably small for departures of 1 percent or less, as indicated by sphere traverses behind the 5-inch screen previously described.

DISCUSSION

The relationship exhibited in figure 18 shows that a given small percentage change in the intensity of the turbulence produces approximately the same effect as a change of five times as much in the scale of the turbulence. Since the diameter of the sphere enters into the ordinate, the critical Reynolds Number depends on the diameter, but here also it requires a percentage change in diameter approximately five times as great as in the intensity of the turbulence to produce the same effect.

It is of some interest to inquire whether the ratio of the values of the critical Reynolds Number for two air streams depends on the diameter of the sphere used. The ratio will be independent of diameter if and only if the curve of figure 18 is of the form

$$\frac{\sqrt{\overline{u^2}}}{U}\left(\frac{D}{L}\right)^{1/5} = CR^n{}_{crit}$$

It may be seen by plotting on logarithmic paper that the observations do not fit such a curve except over short distances. Hence if the diameter of the sphere is varied through a sufficiently wide range, the ratio of two values as well as the absolute values of the critical Reynolds Number of the sphere for two air streams will depend on the diameter.

The use of spheres of different diameters in the same air stream does not give a separation of the effects of scale and intensity, since each observation when reduced gives only the value of $\frac{\sqrt{\overline{u^2}}}{U}\left(\frac{1}{L}\right)^{1/5}$. If $\frac{\sqrt{\overline{u^2}}}{U}$ is independently measured, it is theoretically possible to determine L but the precision is very poor because of the small slope of the curve of figure 18 and the presence of the fifth root.

In the presentation of the experimental data and the discussion up to this point, we have regarded the sphere as a turbulence-measuring device that was to be calibrated in terms of the intensity and scale of the turbulence. It is also possible to consider the sphere as a typical object of aerodynamic study and the data as the aerodynamic characteristics of the sphere as a function of turbulence. These data may then give some clue as to the effect of turbulence on other bodies in which the phenomenon of separation is involved.

The first conclusion that may be drawn by inference is that some linear dimension corresponding to the diameter of the sphere enters into the turbulence variable. In the case of an airfoil, the ratio of the chord of the airfoil to the scale of the turbulence would be of importance. If, for example, we consider tests on two similar airfoils of different size in the same air stream and at the same Reynolds Number, the maximum lift coefficient may be expected to differ because of the influence of the scale of the turbulence. This result would be analogous to the different drag or pressure coefficients observed at the same Reynolds Number for spheres of different sizes in the same air stream. Because of the fifth root, and the limits on the possible size variation in a given wind tunnel, the effect will be small and perhaps escape detection. But if a sufficient range of variation is made, the effect will be found.

A second inference is that the effect of turbulence on some other body will not necessarily be the same as that on the sphere. The shape of the curve of figure 18 is undoubtedly related to the pressure distribution characteristics of the sphere and the resulting boundary layer thickness. The pressure distribution over an airfoil will be quantitatively different and the relation between turbulence and the Reynolds Number for transition will be different. Hence if the sphere curves for two air streams are considered to differ only by a shift along the Reynolds Number axis, that is, by a turbulence factor formed from the ratio of the two Reynolds Numbers, and if by analogy curves of maximum lift coefficient in these same two air streams are considered to differ only by a similar turbulence factor, the factors cannot be considered the same for spheres and airfoils or even for two different airfoils. Here again the effects may be small and not readily detected. The concept of turbulence factor as previously defined has been found very useful. Because of the small effect of $\frac{D}{L}$ compared with $\frac{\sqrt{\overline{u^2}}}{U}$, the factor has so far proved to be a sufficiently good approximation in engineering practice although, as we have shown here, it is only an approximation.

IV—THE EFFECT OF WIRE LENGTH IN MEASUREMENTS OF INTENSITY AND SCALE OF TURBULENCE BY THE HOT-WIRE METHOD

In the measurements of intensity and scale of turbulence described in parts I and II, hot wires approximately 5 millimeters long were used, the length being sufficiently great so that air velocity fluctuations on one part of the wire are not completely correlated with those on another part. As will be shown, this lack of correlation causes the root-mean-square voltage fluctuation across the wire to be reduced by an amount

that depends upon the rate of falling off of correlation along the wire. This reduction in root-mean-square voltage fluctuation must be taken into account in all measurements of fluctuating velocities by hot-wire anemometers, including its effect on measurements of the intensity of the turbulence and its effect on measurements of the scale of turbulence.

THE EFFECT OF WIRE LENGTH ON INTENSITY MEASUREMENTS

Suppose a hot wire of length l carrying a constant current to be placed in a turbulent air stream perpendicular to the direction of flow, as in the experimental arrangement for measurements of intensity of turbulence. If the fluctuating potential drop across the wire is fed into an amplifier compensated for the thermal lag of the wire, the output voltage, denoted by e, will be directly proportional to the fluctuations of air speed on the hot wire.[8]

For the case of complete correlation of velocity fluctuations at all points of the wire, the fluctuating output voltage will be given by

$$e_1=Kul$$

where u is the fluctuating air velocity, l the length of the wire, and K a constant of proportionality, depending

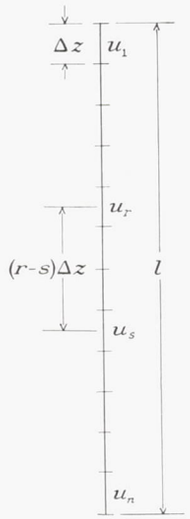

FIGURE 19.—Schematic diagram illustrating nonuniform conditions along the wire as used for measurement of intensity of turbulence.

on the dimensions of the hot wire, its resistivity and temperature coefficient of resistivity, the current through the wire, the mean speed of the air flow, and the amplification.

The output meter on the amplifier (a thermal type milliammeter) gives indications proportional to the mean square of the output voltage, given by

$$\overline{e_1^2}=K^2l^2\overline{u^2} \tag{18}$$

Now consider the case where the velocity fluctuations at various points along the wire are not completely correlated. Let us assume the wire to be divided into n equal segments, each of length Δz, and let the velocity fluctuation of the air passing over any segment be denoted by u_i. (See fig. 19.) For this case the output voltage from the amplifier will be given by

$$e=K\sum_{i=1}^{n}u_i\Delta z$$

and its mean squared value by

$$\begin{aligned}\overline{e^2}&=K^2\Delta z^2\overline{(\Sigma u_1)^2} \qquad (19)\\ &=K^2\Delta z^2[\overline{u_1^2}+\overline{u_2^2}+\overline{u_3^2}+\overline{u_4^2}+\ \ldots\ .+\overline{u_n^2}\\ &\qquad +2\overline{u_1u_2}+2\overline{u_2u_3}+2\overline{u_3u_4}+\ \ldots\ .+2\overline{u_{n-1}u_n}\\ &\qquad +2\overline{u_1u_3}+2\overline{u_2u_4}+\ \ldots\ .+2\overline{u_{n-2}u_n}\\ &\qquad +2\overline{u_1u_4}+\ \ldots\ .+2\overline{u_{n-3}u_n}\\ &\qquad \vdots\\ &\qquad +2\overline{u_1u_n}]\end{aligned}$$

The correlation coefficient R between any two velocity fluctuations, u_r and u_s, is defined as

$$R=\frac{\overline{u_ru_s}}{\sqrt{\overline{u_r^2}}\sqrt{\overline{u_s^2}}}$$

Since the mean square of the velocity fluctuations along the wire is constant

$$\overline{u_r^2}=\overline{u_s^2}=\overline{u^2}$$

$$R=\frac{\overline{u_ru_s}}{\overline{u^2}}$$

Let us assume that the correlation between the velocity fluctuations at any two segments is a function only of the distance between the segments; that is

$$\frac{\overline{u_ru_s}}{\overline{u^2}}=R(\{r-s\}\Delta z)$$

where as in previous parts of the paper, R followed by a quantity in parentheses means the value of R at a distance equal to that quantity. Thus:

$$\begin{aligned}\overline{u_1u_2}=\overline{u_2u_3}=\ \ldots\ .&=\overline{u_{n-1}u_n}=R(\Delta z)\ \overline{u^2}\\ \overline{u_1u_3}=\overline{u_2u_4}=\ \ldots\ .&=\overline{u_{n-2}u_n}=R(2\Delta z)\overline{u^2}\\ \overline{u_1u_4}=\overline{u_2u_5}=\ \ldots\ .&=\overline{u_{n-3}u_n}=R(3\Delta z)\overline{u^2}\\ &\ \ \vdots\\ &\overline{u_1u_n}\ \ =R(\{n-1\}\Delta z)\overline{u^2}\end{aligned}$$

[8] This result is true if the velocity fluctuations are small compared with the mean velocity of flow. (See reference 6.)

Equation (19) thus becomes:

$$\overline{e^2}=K^2\Delta z^2\overline{u^2}\Big[n+2(n-1)R(\Delta z)+2(n-2)R(2\Delta z)+2(n-3)R(3\Delta z)+\ \ldots\ .+2R(\{n-1\}\Delta z)\Big]$$

$$=K^2\overline{u^2}\Big[n\Delta z^2+2n\Delta z\Big\{R(\Delta z)\Delta z+R(2\Delta z)\Delta z+R(3\Delta z)\Delta z+\ \ldots\ .+R(\{n-1\}\Delta z)\Delta z\Big\}$$

$$-2\Big\{\Delta zR(\Delta z)\Delta z+2\Delta zR(2\Delta z)\Delta z+3\Delta zR(3\Delta z)\Delta z+\ \ldots\ .+(n-1)\Delta zR(\{n-1\}\Delta z)\Delta z\Big\}\Big]$$

Now let the number of segments n increase indefinitely, and the length of each segment Δz approach zero, in such a way that the product $n\Delta z$ is always equal to the length of the wire l. Passing to the limit, we have

$$\overline{e^2}=K^2\overline{u^2}\Big[2l\int_0^l R(z)dz-2\int_0^l zR(z)dz\Big]$$

$$=2K^2\overline{u^2}\int_0^l (l-z)R(z)dz \qquad (20)$$

Comparing this expression with equation (18), the effect of the incomplete correlation of velocity fluctuations at different points on the wire is to reduce the mean square fluctuation voltage and thus the meter reading in the ratio K_1^2, given by

$$K_1^2=\frac{\overline{e_1^2}}{\overline{e^2}}=\frac{l^2}{2\int_0^l (l-z)R(z)dz} \qquad (21)$$

In the calculations of intensity of turbulence described in part II, the square root of the output meter reading enters as a multiplying factor. Thus, to obtain the true value for the intensity of turbulence, the calculated values must be multiplied by the factor K_1, given by equation (21). In order to obtain numerical values for K_1, $R(z)$ must be known as a function of z.

THE EFFECT OF WIRE LENGTH ON SCALE MEASUREMENTS

Let us now consider the effect of incomplete correlation of velocity fluctuations at different points of the wire on measurements of the correlation of velocity fluctuations, as described in part I. Suppose two wires A and B, each of length l and carrying a constant current, be placed in a turbulent air stream, parallel to one another, a distance apart y, and in a plane perpendicular to the direction of flow. (See fig. 20.)

Let us assume each wire to be divided into n segments, each of length Δz, and let the velocity fluctuation on any segment of A be denoted by u_i, and of B by v_i. As in the previous discussion, the fluctuating output voltage across each wire will be given by:

$$e_A=K\sum_{i=1}^{n}u_i\Delta z$$

$$e_B=K\sum_{i=1}^{n}v_i\Delta z$$

The correlation between the voltage fluctuations e_A and e_B will obviously be a function of y. Let us then define a correlation coefficient $R'(y)$, representing the correlation between the voltage fluctuations of wires A and B, placed a distance y apart. Thus, by definition, $R'(y)$ is given by

$$R'(y)=\frac{\overline{e_A e_B}}{\sqrt{\overline{e_A}^2}\sqrt{\overline{e_B}^2}}$$

Making use of the foregoing equations and of the fact that the mean square of the velocity fluctuations is the same at the two wires, we have:

$$R'(y)=\frac{K^2\Delta z^2\overline{(\Sigma u_i)(\Sigma v_i)}}{K^2\Delta z^2\sqrt{\overline{(\Sigma u_i)^2}}\sqrt{\overline{(\Sigma v_i)^2}}}=\frac{\overline{(\Sigma u_i)(\Sigma v_i)}}{\overline{(\Sigma u_i)^2}} \qquad (22)$$

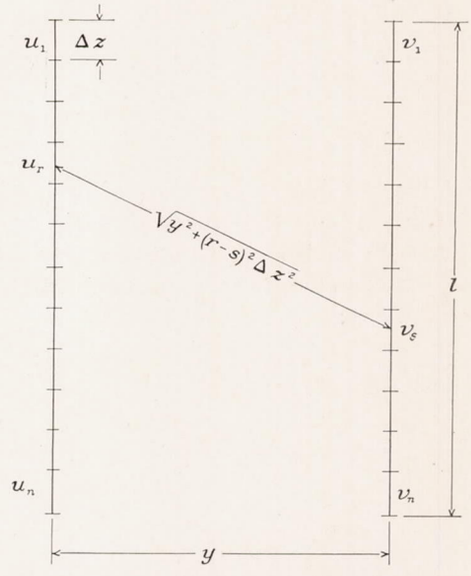

FIGURE 20.—Schematic diagram illustrating nonuniform conditions along two wires as used for measurement of scale of turbulence.

$R'(y)$ may be obtained experimentally as described in part I. Now

$$\begin{aligned}\overline{(\Sigma u_i)(\Sigma v_i)}\Delta z^2=\Delta z^2[&\overline{u_1v_1}+\overline{u_2v_2}+\overline{u_3v_3}+\ \ldots\ .+\overline{u_nv_n}\\&+\overline{u_1v_2}+\overline{u_2v_3}+\ \ldots\ .+\overline{u_{n-1}v_n}\\&+\overline{u_2v_1}+\overline{u_3v_2}+\ \ldots\ .+\overline{u_nv_{n-1}}\\&+\overline{u_1v_3}+\ \ldots\ .+\overline{u_{n-2}v_n}\\&+\overline{u_3v_1}+\ \ldots\ .+\overline{u_nv_{n-2}}\\&\qquad\vdots\\&\qquad\vdots\\&+\ \overline{u_1v_n}\\&+\ \overline{u_nv_1}]\end{aligned}$$

Now let us assume that the correlation of the velocity fluctuations at any segment of A with that at any

segment of B is a function only of the distance between the segments. That is,

$$\frac{\overline{u_r v_s}}{\overline{u^2}} = R(\sqrt{(r-s)^2\Delta z^2 + y^2})$$

Thus:

$$\overline{u_1 v_1} = \overline{u_2 v_2} = \overline{u_3 v_3} = \ldots = \overline{u_n v_n} = R(y)\overline{u^2}$$

$$\overline{u_1 v_2} = \overline{u_2 v_3} = \overline{u_3 v_4} = \ldots = \overline{u_{n-1} v_n}$$

$$= \overline{u_2 v_1} = \overline{u_3 v_2} = u_4 v_3 = \ldots = \overline{u_n v_{n-1}} = R(\sqrt{(\Delta z)^2 + y^2})\overline{u^2}$$

$$\overline{u_1 v_3} = \overline{u_2 v_4} = \overline{u_3 v_5} = \ldots = \overline{u_{n-2} v_n}$$

$$= \overline{u_3 v_1} = \overline{u_4 v_2} = \overline{u_5 v_3} = \ldots = \overline{u_n v_{n-2}} = R(\sqrt{(2\Delta z)^2 + y^2})\overline{u^2}$$

$$\vdots$$

$$\overline{u_1 v_n} = \overline{u_n v_1} = R(\sqrt{(n-1)^2\Delta z^2 + y^2})\overline{u^2}$$

$$\overline{(\Sigma u_i)(\Sigma v_i)}\Delta z^2 = \overline{u^2}\Delta z^2\Big[nR(y) + 2(n-1)R(\sqrt{(\Delta z)^2+y^2}) + 2(n-2)R(\sqrt{(2\Delta z)^2+y^2}) + 2(n-3)R(\sqrt{(3\Delta z)^2+y^2})$$

$$+ \ldots . + 2R(\sqrt{(n-1)^2\Delta z^2 + y^2})\Big]$$

$$= \overline{u^2}\Big[n\Delta z^2 R(y) + 2n\Delta z\Big\{R(\sqrt{\Delta z^2+y^2})\Delta z + R(\sqrt{(2\Delta z)^2+y^2})\Delta z + R(\sqrt{(3\Delta z)^2+y^2})\Delta z + \ldots .$$

$$+ R(\sqrt{(n-1)^2\Delta z^2+y^2})\Delta z\Big\} - 2\Big\{\Delta z R(\sqrt{(\Delta z)^2+y^2})\Delta z + 2\Delta z R(\sqrt{(2\Delta z)^2+y^2})\Delta z + 3\Delta z R(\sqrt{(3\Delta z)^2+y^2})\Delta z +$$

$$\ldots . + (n-1)\Delta z R(\sqrt{(n-1)^2\Delta z^2+y^2})\Delta z\Big\}\Big]$$

Now let the number of segments of each wire n increase indefinitely and the length of each segment Δz approach zero in such a way that the product $n\Delta z$ is always equal to the length of each wire, l. Passing to the limit, we have:

$$\overline{(\Sigma u_i)(\Sigma v_i)}\Delta z^2$$

$$= \overline{u^2}\Big[2l\int_0^l R(\sqrt{z^2+y^2})dz - 2\int_0^l zR(\sqrt{z^2+y^2})dz\Big]$$

$$= 2\overline{u^2}\int_0^l (l-z)R(\sqrt{z^2+y^2})dz$$

From equations (19) and (20)

$$\overline{(\Sigma u_i)^2}\Delta z^2 = 2\overline{u^2}\int_0^l (l-z)R(z)dz$$

Thus equation (22) becomes

$$R'(y) = \frac{\int_0^l (l-z)\,R(\sqrt{z^2+y^2})dz}{\int_0^l (l-z)R(z)dz} \tag{23}$$

The scale of the turbulence L has been defined as the integral

$$L = \int_0^\infty R(y)dy \tag{24}$$

Let us denote by L' the following integral:

$$L' = \int_0^\infty R'(y)dy$$

L' may be determined experimentally as described in Part I, and L may be found by dividing L' by a factor K_2, defined as

$$K_2 = \frac{L'}{L} \tag{25}$$

If $R(y)$ is a known function of y, the integrations expressed in equations (23) and (24) may be performed, and numerical values of K_2 computed.

CALCULATION OF FACTORS FOR APPLICATION TO EXPERIMENTAL RESULTS

It may be seen from equation (23) that the shorter the wires used and the more slowly $R(z)$ varies with z, the more nearly will the right-hand member of this equation approach R(y). Thus curves of $R'(y)$ obtained under conditions where L is much larger than l, resulting either from large scale of the turbulence or the use of short wires, should indicate the character of the function $R(y)$.

In figure 21 are shown observed values of $R'(y)$ representing the average of eight traverses at 200 inches behind the 5-inch-mesh screen where the foregoing conditions are most nearly fulfilled. These points are seen to lie closely to the curve, which is an exponential curve represented by the equation

$$R'(y) = e^{-\frac{y}{L'}}$$

where L' is the uncorrected scale of the turbulence. Since the correction is small, let us assume that $R(y)$ is given by

$$R(y) = e^{-\frac{y}{L}} \tag{26}$$

and determine what form will be taken by $R'(y)$ and what values will be obtained for K_1 and K_2.

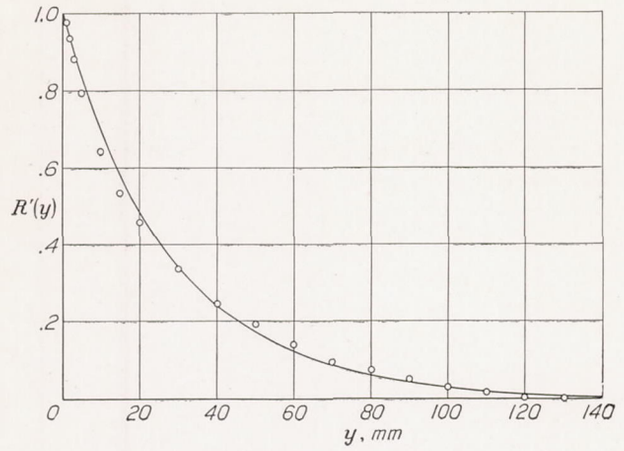

FIGURE 21.—Observed correlation coefficient as a function of y. Points, average of 8 traverses at 200 inches behind 5-inch screen; curve, plot of $R'=e^{-\frac{y}{L'}}$.

Equation (23) becomes

$$R'(y)=\frac{\int_0^l (l-z)e^{-\frac{\sqrt{z^2+y^2}}{L}}dz}{\int_0^l (l-z)e^{-\frac{z}{L}}dz} \tag{27}$$

The factor K_1, given by equation (21) becomes

$$K_1=\frac{l}{\sqrt{2\int_0^l (l-z)e^{-\frac{z}{L}}dz}} \tag{28}$$

and K_2, given by equation (25) becomes

$$K_2=\frac{1}{L}\int_0^\infty R'(y)dy \tag{29}$$

It is convenient to write these equations in nondimensional form, changing to the new variables

$$r=\frac{y}{l},\ s=\frac{z}{l},\ c=\frac{l}{L}$$

In this notation equation (28) becomes

$$K_1=\frac{1}{\sqrt{2\int_0^1 (1-s)e^{-cs}ds}}=\frac{c}{\sqrt{2(e^{-c}-1+c)}} \tag{30}$$

Equation (27) becomes

$$R'(r)=\frac{\int_0^1 (1-s)e^{-c\sqrt{r^2+s^2}}ds}{\int_0^1 (1-s)e^{-cs}ds}$$

$$=2K_1^2\int_0^1 (1-s)e^{-c\sqrt{r^2+s^2}}ds \tag{31}$$

Equation (31) is not directly integrable but may be evaluated for large values of r by expansion in a power series in s^2 and integrating term by term.

Let

$$f(s^2)=e^{-c\sqrt{r^2+s^2}}$$

Expanding f in powers of s^2, equation (31) becomes

$$R'(r)=2K_1^2\int_0^1 (1-s)\left[f(0)+f'(0)s^2+f''(0)\frac{s^4}{2!}+f'''(0)\frac{s^6}{3!}++\cdots\right]ds$$

$$=K_1^2\left[f(0)+\frac{1}{6}f'(0)+\frac{1}{30}f''(0)+\frac{1}{168}f'''(0)+\cdots\right]$$

Evaluating the terms in this series

$$f(0)=e^{-cr}$$

$$f'(0)=-\frac{ce^{-cr}}{2r}$$

$$f''(0)=+\frac{c(1+cr)e^{-cr}}{4r^3}$$

$$f'''(0)=-\frac{c(3+3cr+c^2r^2)e^{-cr}}{8r^5}$$

Equation (31) then becomes

$$R'(r)=K_1^2e^{-cr}\left[1-\frac{c}{12\,r}+\frac{c(1+cr)}{120\,r^3}-\frac{c\left(1+cr+\frac{c^2r^2}{3}\right)}{448\,r^5}+\cdots\right] \tag{32}$$

The first four terms of this series will give values of $R'(r)$ with sufficient accuracy for $r>1$. For smaller values of r, a series containing positive powers of r must be obtained.

Rewriting equation (31)

$$R'(r)=2K_1^2\left[\int_0^1 e^{-c\sqrt{r^2+s^2}}ds-\int_0^1 s\,e^{-c\sqrt{r^2+s^2}}ds\right]$$

The second integral can be evaluated directly

$$\int_0^1 s\,e^{-c\sqrt{r^2+s^2}}ds=\frac{1}{c^2}\left[e^{-cr}(1+cr)-e^{-c\sqrt{r^2+1}}(1+c\sqrt{r^2+1})\right]$$

The first integral may be evaluated by expanding the integrand in a series of powers of $c\sqrt{r^2+s^2}$.

$$\int_0^1 e^{-c\sqrt{r^2+s^2}}ds=\int_0^1\left[1-c(r^2+s^2)^{1/2}+\frac{c^2}{2!}(r^2+s^2)-\frac{c^3}{3!}(r^2+s^2)^{3/2}+\ldots.\right]ds$$

Let $I_n(r)=\int_0^1 (r^2+s^2)^{n/2}ds$. We then have

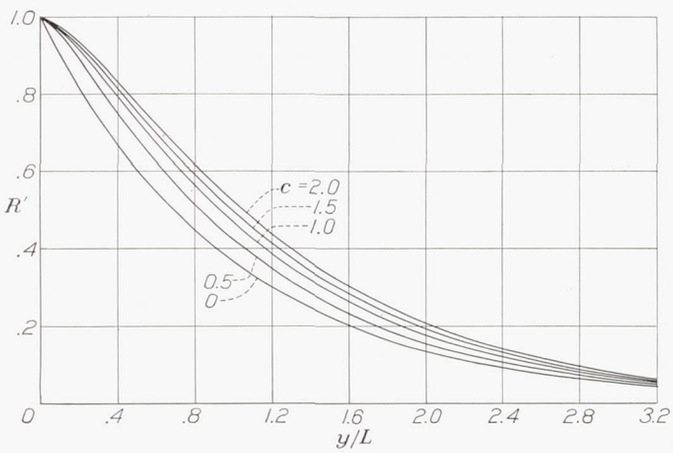

FIGURE 22.—Theoretical values of R and of R' as a function of cr or y/L for various values of c.

$$R'(r)=2K_1^2\left[\frac{e^{-c\sqrt{r^2+1}}}{c^2}(1+c\sqrt{r^2+1})-\frac{e^{-cr}(1+cr)}{c^2}+I_0(r)-cI_1(r)+\frac{c^2}{2!}I_2(r)-\frac{c^3}{3!}I_3(r)+\frac{c^4}{4!}I_4(r)+\ldots.\right] \quad (33)$$

$I_n(r)$ may be computed from the following recurrence formula:

$$I_n(r)=\frac{(r^2+1)^{n/2}}{n+1}+\frac{n\,r^2}{n+1}I_{n-2}(r)$$

where $I_o(r)=1$

$$I_1(r)=\frac{(r^2+1)^{1/2}}{2}+\frac{r^2}{2}\sinh^{-1}\frac{1}{r}$$

In figure 22 is shown a curve of $R(c=0)$ and of R' as a function of $cr(=y/L)$ for various values of c. It is seen that the effect of the incomplete correlation of velocity fluctuations along the wires is to make the observed correlation too large at large values of r by a factor K_1^2 (see equation 32), and to change the shape of the curve for small values of r.

In figure 23 are shown some experimental curves of $R'(y)$ as a function of y/M for different ratios of the length of the hot wire to the scale of the turbulence, that may be compared to the curves of figure 22. The similarity of these two sets of curves can be noted.

Let us now consider the effect of incomplete correlation of velocity fluctuations along the hot wires on the value of L' obtained by integration of the experimental $R'(y)$ curves. Writing equation (29) in terms of r instead of y

$$K_2=\frac{l}{L}\int_0^\infty R'(r)dr \quad (34)$$

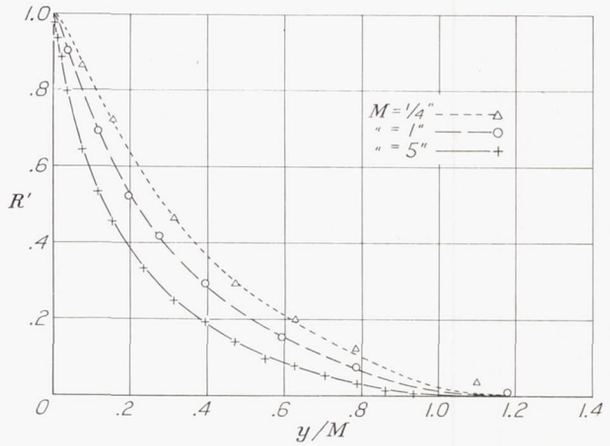

FIGURE 23.—Experimental values of $R'(y)$ for various values of y/M for comparison with figure 22.

This integral may be evaluated by graphical integration of $R'(r)$ calculated from equation (32) and (33), or as follows: Substituting (31) in (34)

$$K_2=2K_1^2c\int_0^\infty\int_0^1(1-s)e^{-c\sqrt{r^2+s^2}}dsdr$$

Transforming this surface integral into polar coordinates, by the transformations

$$r=\rho\cos\theta \qquad s=\rho\sin\theta \qquad dsdr=\rho d\rho d\theta$$

$$K_2=2K_1^2c\int_0^{\pi/2}\int_0^{\csc\theta}(1-\rho\sin\theta)e^{-c\rho}\rho d\rho d\theta$$

Integrating with respect to ρ:

$$K_2=2K_1^2c\int_0^{\pi/2}\left[\frac{1}{c^2}+\frac{e^{-c\csc\theta}}{c^2}+\frac{2\sin\theta e^{-c\csc\theta}}{c^3}-\frac{2\sin\theta}{c^3}\right]d\theta$$

$$K_2=\frac{2K_1^2}{c^2}\left[\frac{\pi}{2}c-2+c\int_0^{\pi/2}e^{-c\csc\theta}\left(1+\frac{2}{c\csc\theta}\right)d\theta\right]$$

Let $J(c)=\int_0^{\pi/2}e^{-c\csc\theta}\left(1+\frac{2}{c\csc\theta}\right)d\theta$

$$K_2=\frac{\frac{\pi}{2}c-2+cJ(c)}{e^{-c}-1+c} \quad (35)$$

The integral $J(c)$ cannot be evaluated directly but may be expanded in an asymptotic series, which will give $J(c)$ for sufficiently large values of c. For small values of c, however, it is most easily evaluated by Simpson's rule.

Table VIII gives values of K_1 and K_2 as a function of $c\left(=\frac{l}{L}\right)$ computed from equations (30) and (35). Curve A of figure 24 shows K_2 plotted as a function of $\frac{l}{L}$. Curve B shows K_2 as a function of $\frac{l}{L'}$, and is obtained from curve A by dividing the abscissa of a given point on A by the ordinate of that point and then plotting that ordinate above the new abscissa obtained. Curve B is used for the correction of the experimental data on correlation of velocity fluctuations. The procedure is as follows: The area under the experimental curves of R' as a function of y is obtained, from which is found L'. The ratio of l, the length of the hot wires, to L' is calculated and from curve B, figure 24, the factor K_2 is found. L' is then divided by K_2 to obtain L.

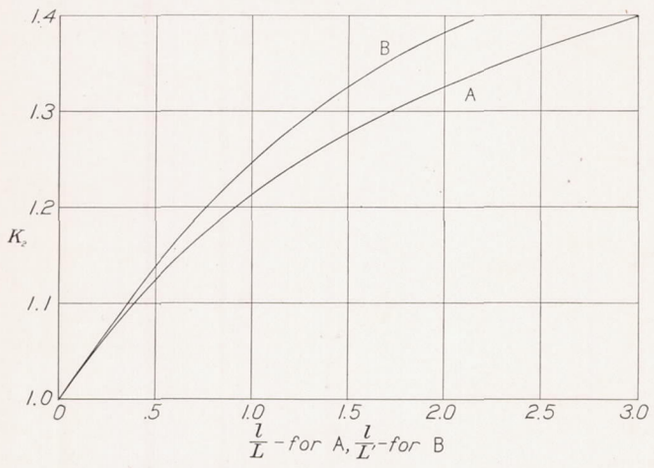

FIGURE 24.—The factor K_2 as a function of l/L and l/L'.

The numerical values obtained for the correction factors K_1 and K_2 depend, of course, on the assumption that R may be represented by equation (26), and thus can be expected to be accurate only in so far as equation (26) represents the true variation of correlation with distance. It is seen from figure 21 that there is a tendency for R or R' to fall off initially more rapidly with distance than the exponential relation until the correlation falls to about 0.3, and then less rapidly, finally falling to zero instead of approaching zero asymptotically.

The correction factors thus computed can be considered only as approximations, and more accurate determination of the variation of the correlation coefficient R with distance, especially for small distances, is needed in order to improve materially their accuracy.

V—VARIATION OF CORRELATION COEFFICIENT WITH FREQUENCY CHARACTERISTICS OF THE MEASURING APPARATUS AND WITH AZIMUTH

In the development of the experimental technique for measuring the scale of the turbulence, certain unexpected phenomena were encountered. These phenomena were studied to only a limited extent, usually only with regard to their bearing on the measurement of the scale of the turbulence as previously defined. The incidental and incomplete studies of these phenomena give additional information as to the characteristics of turbulent flow and since we cannot at present pursue these studies further, the information obtained is placed on record for the benefit of others who may wish to do so.

EFFECT OF COMPENSATION FOR LAG OF WIRE

In our first measurements of the correlation coefficient, no compensation was made for the lag of the wire. We erroneously assumed that, if the two wires were identical in every respect including lag, there would be no effect of the lag on the value of the correlation coefficient. Fortunately, the actual experiment was tried and it was discovered that the introduction of compensation had a very large effect. Two typical comparisons are shown in figure 25. When no compensation was used, the observed correlation coefficient fell off much more slowly with the separation of the wires. As a result, the observed scale L' was much greater. For example, for the 1-inch screen at a distance of 40 mesh lengths, the observed $\frac{L'}{M}$ without compensation was 0.602 as compared with 0.308 obtained with proper compensation, an error of nearly 100 percent. Similarly for the 3¼-inch screen at a distance of 41 mesh lengths, the observed $\frac{L'}{M}$ without compensation was 0.464 as compared with 0.236 obtained with proper compensation. The difference in a number of comparisons at different distances was always greater than 50 percent.

Since the presence or absence of compensation corresponds simply to different frequency characteristics of the measuring apparatus, it was inferred that the results indicated a variation of the correlation coefficient with frequency, the disturbances of lower frequency being correlated over greater distances than the disturbances of higher frequency.

CROSS-STREAM CORRELATION FOR VARIOUS FREQUENCY BANDS

Measurements were made with a set of electric filters to study the correlation for various frequency bands. The compensating circuit was used, so that the results represent, as closely as can be obtained, the variation of the correlation with frequency. The available filters were high- and low-pass filters designed for connection as band-pass filters. The nominal frequency bands were 0–250, 250–500, 500–1500, 1500–3000, and 3000–∞ cycles per second. Ideal filters would give a uniform transmission within the band and no transmission outside the band. The actual characteristics are shown in figure 26. Although extremely good for acoustic measurements, the filters are far from ideal for the present purpose.

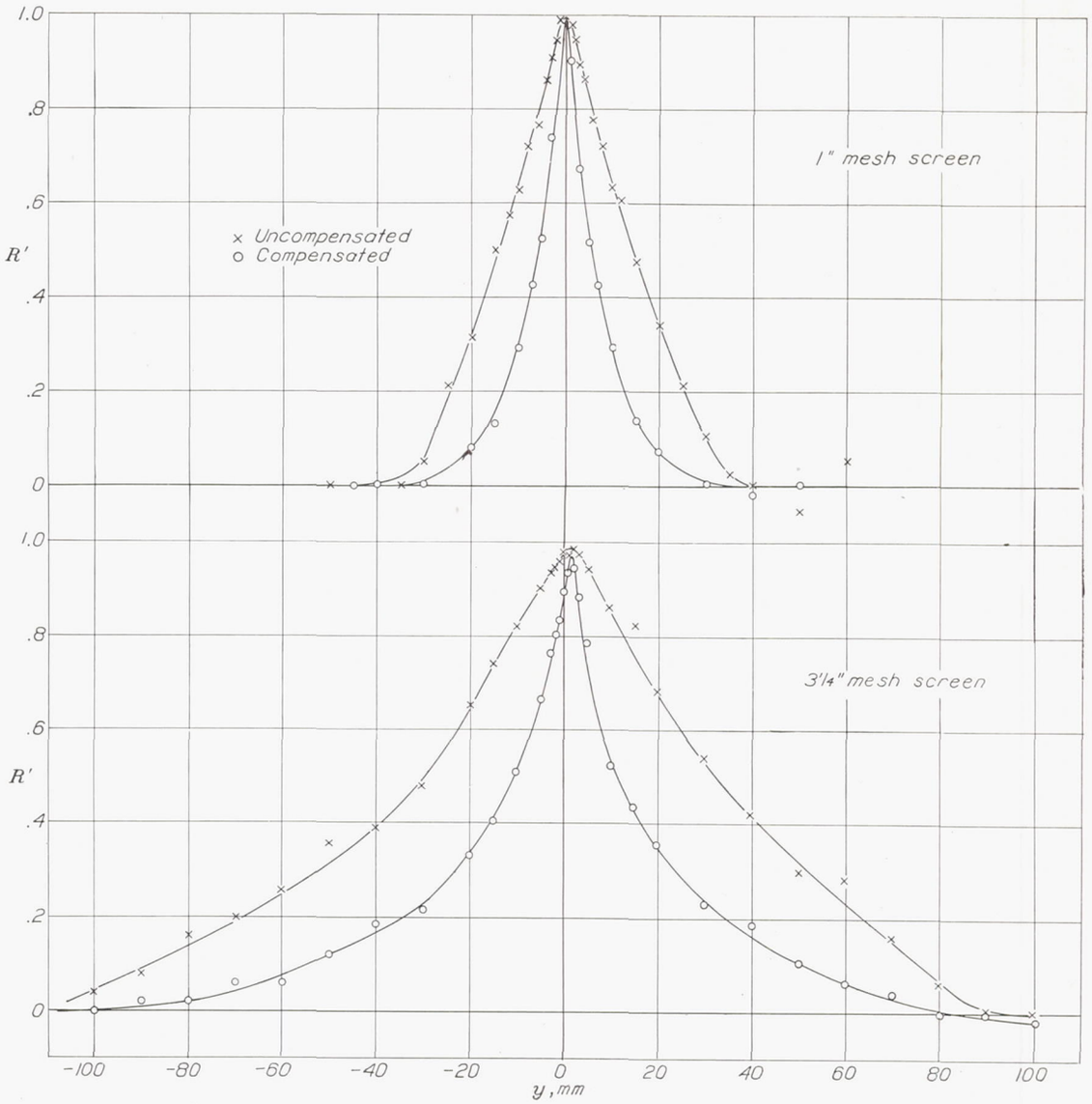

FIGURE 25.—Correlation curves showing effect of compensation. Curves for 1-inch mesh observed at 40 mesh lengths aft. Curves for 3¼-inch mesh observed at 41-mesh lengths aft.

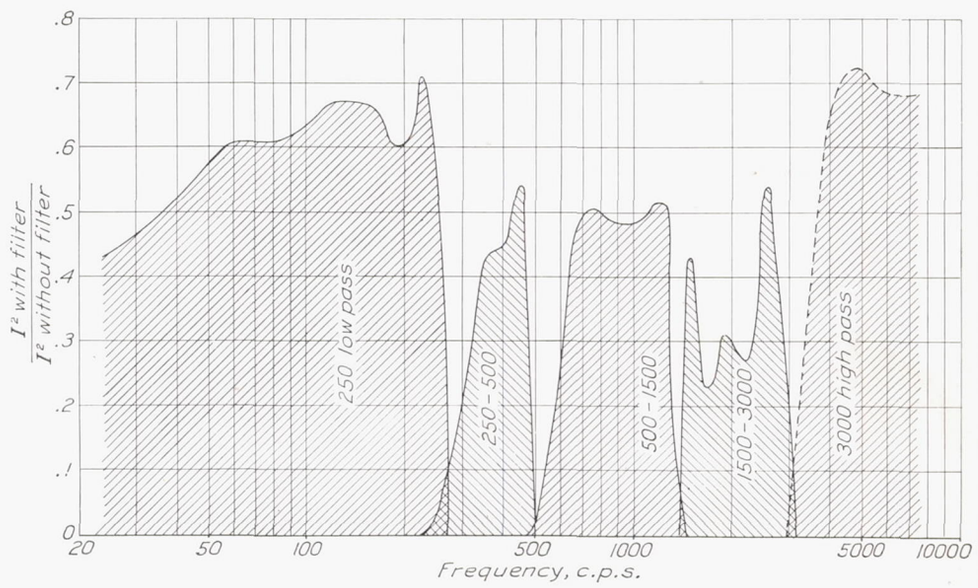

FIGURE 26.—Frequency characteristics of filters.

Measurements of correlation were made at a distance of 40 mesh lengths behind the 1-inch screen at speeds of 20 and 40 feet per second for the bands 0–250, 250–500, 500–1500. The intensity in the two higher bands was so small that satisfactory measurements could not be made. The results are shown in figure 27. The large effect of frequency is obvious. In the 500–1500 band negative correlations are observed, indicating that for frequencies in this band an increase in speed at one wire tends to be associated with a decrease in speed at the other. No attempt was made to correct these observations for the finite length of the wires. Some idea of the magnitude of the effect can be obtained from figure 5. The application of the corrections would not change the general picture.

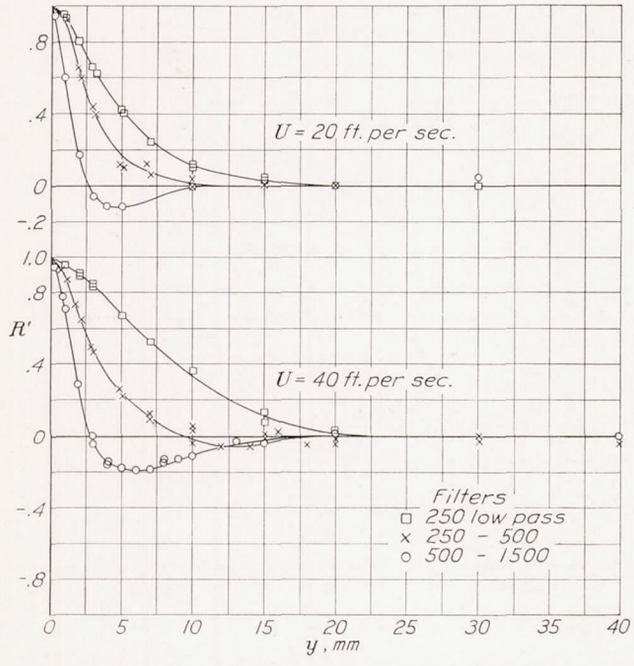

FIGURE 27.—Correlation curves corresponding to several frequency bands. 1-inch screen, 40 mesh lengths aft.

A rough analysis of the distribution of the intensity of the turbulence with frequency was made by means of the filters for a distance of 26 mesh diameters from the 1-inch screen. The results are shown in table IX. The analysis is rough because of the variation of the attenuation of the filters with frequency. Allowance has been made for the differences in average attenuation. The change in the distribution with the change in mean speed is consistent with the assumption that the fluctuations at a point are the result of a pattern of eddy motion in space that is carried along with the mean speed of the stream and changes but little as the mean flow travels a distance of a few centimeters. One may consider the eddy system from the point of view of a stationary observer, in which case it may be described by giving the statistical distribution of intensity with frequency. Or one may consider the system from the point of view of an observer moving with the stream, in which case the system may be described by giving the statistical distribution of intensity with wave length. A wave length λ in the second picture corresponds to a frequency f in the first equal to U/λ, where U is the mean speed. If the statistical distribution of intensity with wave length in space is independent of mean speed, the distribution of intensity with frequency when the pattern is observed at a fixed point is shifted toward higher frequencies as the mean speed is increased. The filter bands are so wide that no complete analysis can be made. It is seen, however, in figure 27, that for a given frequency band the correlation falls off more rapidly with distance at 20 feet per second than at 40 feet per second. The same frequency band corresponds to shorter wave lengths at 20 feet per second than at 40 feet per second. For example, the 250–500 filter used in a stream of mean speed 20 feet per second (610 centimeters per second) selects wave lengths of 1.22 to 2.44 centimeters, whereas in a stream of 40 feet per second (1,220 centimeters per second), the same filter selects wave lengths from 2.44 to 4.88 centimeters. When no filter and no compensation are used, the apparatus weights the various frequencies according to the law $\frac{1}{\sqrt{1+A^2f^2}}$, where f is the frequency and A is a lag constant of the wire. For this condition the correlation falls off less rapidly than for the 0–250 filter.

Experiment shows that, if the apparatus does not weight all frequencies uniformly, the observed correlation curve varies with the mean speed; but, if the frequency compensation is correct, the observed correlation curve is independent of the mean speed. This experimental result is again consistent with the hypothesis that a fixed eddy pattern independent of mean speed is transported past the measuring apparatus at the mean speed. The frequency pattern then varies with the speed. If the apparatus responds uniformly to all frequencies, there will be no effect of mean speed; but, if there is frequency distortion, apparent variations with mean speed will be introduced.

ALONG-STREAM CORRELATION

In order to avoid troublesome constant errors in the measurement of the distance between the two wires of the correlation apparatus, it was decided to allow one wire to travel behind the other with a clearance of a few tenths of a millimeter, so that measurements could be taken on both sides, the zero position being located by the wake disturbance of the upstream wire. This procedure introduces an error whose magnitude was estimated by studying the correlation along the stream direction. Figure 28 gives a comparison between the correlation coefficients transverse and parallel to the stream at 25½ inches behind the 1-inch screen at 40 feet per second. The correlation falls off more slowly along the stream. From these data it may be estimated that the peaks of the correlation curves are somewhat reduced, the maximum being reduced by about 5 percent

when the clearance is 0.3 millimeter and the scale of the turbulence is as small as 5 millimeters. The effect on the determination of the scale of the turbulence is entirely negligible, but this factor adds to the effects of finite wire length and the noise level of the amplifier to make impossible the studies of the curvature near the peak of the curve, which are desired in connection with Taylor's theory.

The effect of frequency characteristics of the measuring apparatus was also studied for the along-stream correlation. The results at 25½ inches behind the 1-inch screen are plotted in figure 29. These curves are very suggestive. We have already stated that the filters select a given band of wave lengths, the 250–500 filter selecting a mean wave length of 1.83 centimeters at 20 feet per second and 3.66 centimeters at 40 feet per second. These values agree remarkably well with the "wave lengths" exhibited by the correlation curves along stream. The high negative correlations indicate a high degree of "coherence", the fluctuation at the

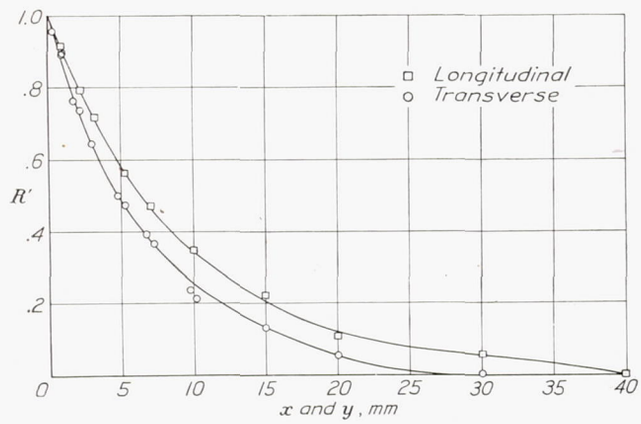

FIGURE 28.—Comparison of transverse and longitudinal correlation. 1-inch-mesh screen, 25-½ mesh lengths aft. Wind speed 40 ft./sec.

upstream wire being repeated a short time later at the downstream wire. It appears probable that if it were possible to make the measurements with a very narrow frequency band, the correlation would vary several times between +1 and −1 as the along-stream separation were increased.

Taylor predicted a relation between the transverse and longitudinal correlation in isotropic turbulence, namely, that the correlation coefficient R varied with the azimuth θ according to the law

$$1-R=(1-R_T)\ (\sin^2\ \theta+\frac{1}{2}\cos^2\ \theta)$$

where R_T is the transverse correlation coefficient.[9]

The longitudinal correlation R_L is then given by the relation

$$2(1-R_L)=(1-R_T)$$

The results of figure 28 do not confirm this relation, since the ratio of $1-R_T'$ to $1-R_L'$ at $y=2$ mm is more nearly 1.4. For smaller or larger values of y, the ratio is less. It does not appear that the correction for finite wire length as computed in part IV would alter this result by more than 10 percent.

In order to study the matter further, the little rotating holder suggested by Taylor (reference 5) was constructed and attention confined to measurements of the ratio. Some results taken with and without the filters

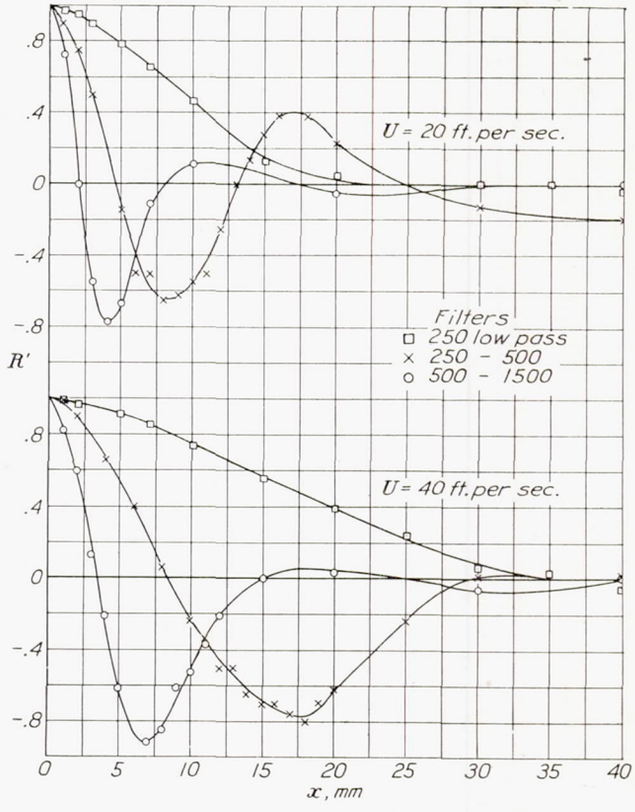

FIGURE 29.—Correlation curves observed along stream corresponding to several frequency bands. 1-inch mesh screen, 25½ inches aft.

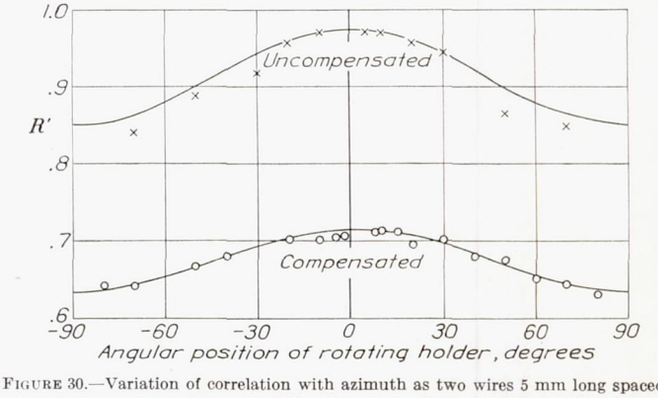

FIGURE 30.—Variation of correlation with azimuth as two wires 5 mm long spaced 9 mm apart are rotated from a position along stream (zero angle) to a position across stream (90° angle).

with wires 2 millimeters apart at 25½ inches behind the 1-inch screen are shown in table X. The ratio varies markedly with frequency and for a given filter with mean speed, as would be expected from figure 29. The value with no filter was about 1.4.

A few measurements with a 9-millimeter spacing of the wires at 38 mesh lengths behind the 3¼-inch screen

[9] In reference 5, the sin and cos of this equation are interchanged.

are shown in figure 30. The curves represent the relation $1-R'=0.150\ (\sin^2\theta+\frac{1}{6}\cos^2\theta)$ for the uncompensated run and $1-R'=0.365\ (\sin^2\theta+\frac{1}{1.28}\cos^2\theta)$ for the compensated run. Here again for the uncompensated run $1-R'$ changes by a factor greater than the theoretical factor 2 between $\theta=0$ and $\theta=90°$ and for the compensated run, less than 2.

This departure from Taylor's theory might be considered an evidence of departure from isotropy but the evidence previously presented as to agreement of values from hot-wire measurements and from measurements of thermal diffusion indicates that such is not the case.

Another possibility is that some systematic experimental error has been overlooked or that the theory of correction for wire length is not based on valid assumptions. The few measurements recorded in this section show that the correlation curves vary with the frequency of the fluctuations considered. Hence the effect of finite wire length is different in different frequency bands, producing a frequency weighting in the apparatus that has been shown to have considerable effect on the observed correlation. The effect would be to suppress the higher frequencies and hence to increase the correlation coefficient at a given separation of the two wires. The magnitude of the increase would be greatest where the scale of the turbulence is least. Such an effect, if of sufficient magnitude, would account for the failure to obtain a single curve of $\frac{L}{M}$ against $\frac{x}{M}$ in figure 7, part I, the curves for small screens being too high. It is also possible that such an effect accounts for the departure of $\frac{1-R_T'}{1-R_L'}$ from the theoretical value 2, since the observed value R_T' would be larger than the true value R_T by a greater amount than R_L' is larger than R_L. The required effects are, however, of such magnitude as to make this explanation seem unreasonable, since the departure from a uniform frequency weighting is small. No adequate theory can be developed without more information as to the variation with frequency. The experimental problem is one of great difficulty since, even if filters of requisite selectivity were available, the further subdivision of the available energy into narrow frequency bands would require still further amplification to make measurements possible.

CONCLUSIONS

The results obtained may be summarized as follows:

1. The scale or "average eddy size" of turbulence may be obtained from the measurement of correlation between speed fluctuations. Such measurements may be made with the same apparatus used to measure the intensity of the turbulence, modified slightly to accommodate two hot wires.

2. A knowledge of the variation of correlation with distance across the stream makes possible a correction of the error introduced in hot-wire results by the lack of complete correlation over the length of the wire. Convenient methods for applying these corrections are presented.

3. Screens are suitable devices for producing turbulence in wind tunnels. The scale of the turbulence is controlled by some dimension of the screen. Since geometrically similar screens were used in the present study, it has not been determined whether mesh or wire size is the controlling factor. The scale of the turbulence produced by a screen increases with distance from the screen.

4. The intensity of the turbulence decreases with distance from the screen, the decay being given by a logarithmic law when the scale of the turbulence increases linearly.

5. The pressure sphere described herein has been found a convenient device for measuring the aerodynamic effect of turbulence. A pressure coefficient of 1.22 corresponds approximately to a drag coefficient of 0.3. Either coefficient will serve to connect a critical Reynolds Number with the effect of turbulence.

6. The critical Reynolds Number of spheres depends on the scale of the turbulence as well as on its intensity. The combined effects may be expressed by

$$R_{crit}=f\left(\frac{\sqrt{\overline{u^2}}}{U}\left[\frac{D}{L}\right]^{1/5}\right)$$

NATIONAL BUREAU OF STANDARDS,
WASHINGTON, D. C., *August 6, 1936.*

REFERENCES

1. Dryden, H. L., and Kuethe, A. M.: Effect of Turbulence in Wind Tunnel Measurements. T. R. No. 342, N. A. C. A., 1930.
2. Dryden, Hugh L.: Reduction of Turbulence in Wind Tunnels. T. R. No. 392, N. A. C. A., 1931.
3. Millikan, C. B., and Klein, A. L.: The Effect of Turbulence. Aircraft Eng., August 1933, pp. 169–174.
4. Bacon, D. L., and Reid, E. G.: The Resistance of Spheres in Wind Tunnels and in Air. T. R. No. 185, N. A. C. A., 1924.
5. Taylor, G. I.: Statistical Theory of Turbulence. Proc. Roy. Soc. of London, series A, vol. 151, no. 873, September 2, 1935, pp. 421–478.
6. Dryden, H. L., and Kuethe, A. M.: The Measurement of Fluctuations of Air Speed by the Hot-Wire Anemometer. T. R. No. 320, N. A. C. A., 1929.
7. Mock, W. C., Jr., and Dryden, H. L.: Improved Apparatus for the Measurement of Fluctuations of Air Speed in Turbulent Flow. T. R. No. 448, N. A. C. A., 1932.
8. Taylor, G. I.: Diffusion by Continuous Movements. Proc. London Math. Soc., vol. 20, August 1921, pp. 196–211.
9. Schubauer, G. B.: A Turbulence Indicator Utilizing the Diffusion of Heat. T. R. No. 524, N. A. C. A., 1935.
10. Schubauer, G. B., and Dryden, H. L.: The Effect of Turbulence on the Drag of Flat Plates. T. R. No. 546, N. A. C. A., 1935.
11. Prandtl, L.: Der Luftwiderstand von Kugeln. Nachr. d. K. Ges. d. Wissensch., Göttingen, Math. phys. Kl., 1914, p. 177.

12. National Advisory Committee for Aeronautics: Twentieth Annual Report, 1934, pp. 16 and 23.
13. Dryden, Hugh L.: Frontiers of Aerodynamics. Jour. Wash. Acad. Sci., vol. 25, March 1935, p. 101.
14. Platt, Robert C.: Turbulence Factors of N. A. C. A. Wind Tunnels as Determined by Sphere Tests. T. R. No. 558, N. A. C. A., 1936.
15. Hoerner, S.: Tests of Spheres with Reference to Reynolds Number, Turbulence, and Surface Roughness. T. M No. 777, N. A. C. A., 1935.
16. Taylor, G. I.: Statistical Theory of Turbulence. Part V. Proc. Roy. Soc. of London, series A, vol. 156, no. 888, August 1936, p. 307.
17. Ower, E., and Warden, R.: Note on the Use of Networks to Introduce Turbulence into a Wind Tunnel. R. & M. No. 1559, British A. R. C., 1934.

TABLE I.—DIMENSIONS OF SCREENS FOR PRODUCING TURBULENCE

Nominal mesh length, inches	Average measured mesh length, inches	Deviation of individual meshes from average, inches		Average measured wire diameter, inches	Material
		Mean	Maximum		
¼	0.248	±0.010	+0.026 −.023	0.050	Iron wire.
½	.515	.012	+.017 −.025	.096	Iron wire.
1	1.007	.005	+.015 −.015	.196	Iron wire.
3¼	3.285	.068	+.163 −.122	.626	Wooden cylinders.
5	5.016	.021	+.04 −.04	.976	Wooden cylinders.

TABLE II.—SCALE OF TURBULENCE

$\frac{x}{M}$ Distance from screen in mesh lengths	$\frac{L'}{M}$	$\frac{L}{M}$	$\frac{x}{M}$ Distance from screen in mesh lengths	$\frac{L'}{M}$	$\frac{L}{M}$
¼-inch mesh screen			½-inch mesh screen		
18.5	0.276	0.183	27.0	0.306	0.237
41.0	[a].405	.290	27.0	.311	.240
41.0	[a].375	.269	42.3	.338	.266
41.0	[a].365	.263	42.3	.355	.280
41.0	[a].387	.278	56.7	.395	.315
53.0	.464	.342	56.7	.366	.292
84.0	.566	.429	79.5	.494	.406
112.0	.602	.463	79.5	.445	.366
159.0	.864	.702	108.0	.548	.458
159.0	.916	.745	108.0	.518	.434
159.0	.798	.649	171.0	[a].626	.536
161.0	[a].805	.648	171.0	[a].609	.521
161.0	[a].782	.631	171.0	[a].622	.532
161.0	[a].808	.652	171.0	[a].556	.475
161.0	[a].738	.595	171.0	[a].604	.517
161.0	[a].752	.606	172.0	.695	.601
161.0	[a].770	.621	172.0	.673	.582
214.0	.906	.742	226.0	.842	.746
			226.0	.846	.750
			226.0	.822	.728

TABLE II.—SCALE OF TURBULENCE—Continued

$\frac{x}{M}$ Distance from screen in mesh lengths	$\frac{L'}{M}$	$\frac{L}{M}$	$\frac{x}{M}$ Distance from screen in mesh lengths	$\frac{L'}{M}$	$\frac{L}{M}$
1-inch mesh screen			3¼-inch mesh screen		
21.0	0.293	0.248	16.5	[a]0.190	0.175
21.0	.277	.234	16.5	[a].202	.187
28.0	.291	.246	16.6	.172	.156
39.5	.394	.345	26.2	[a].220	.205
39.5	.377	.331	26.2	[a].219	.204
40.0	[a].305	.261	26.5	.253	.237
40.0	[a].314	.269	34.6	.257	.241
40.0	[a].300	.258	34.6	.259	.243
40.0	[a].312	.268	34.8	[a].211	.196
53.0	.413	.363	34.8	[a].212	.197
53.0	.366	.321	39.7	[a].250	.234
53.8	[a].352	.306	39.7	[a].226	.212
53.8	[a].368	.319	40.0	[a].235	.220
53.8	[a].344	.298	40.0	[a].230	.215
53.8	[a].335	.292	40.0	[a].235	.220
53.8	[a].335	.292	40.0	[a].241	.226
53.8	[a].316	.274	40.0	[a].258	.242
53.8	[a].312	.271	50.5	.266	.249
53.8	[a].323	.280	50.5	.242	.226
85.0	.451	.405	50.8	[a].258	.242
85.0	.406	.365	50.8	[a].261	.245
113.0	.520	.468	50.8	[a].248	.233
113.0	.426	.383	61.4	[a].303	.287
113.0	.574	.516	61.4	[a].303	.287
113.0	.480	.433	61.4	[a].281	.266
113.0	.462	.416			
135.5	.512	.461	5-inch mesh screen		
135.5	.486	.438			
135.5	.484	.436			
164.0	.496	.446			
164.0	.470	.423	17.1	[a]0.166	0.156
164.0	.505	.454	17.1	[a].166	.156
164.3	[a].551	.499	17.1	[a].172	.162
164.3	[a].480	.435	22.7	[a].201	.190
164.3	[a].488	.442	22.7	[a].210	.200
164.3	[a].504	.457	22.7	[a].189	.180
164.3	[a].527	.478	33.0	[a].202	.192
164.3	[a].500	.453	33.0	[a].199	.189
			39.9	[a].199	.189
			39.9	[a].203	.193
			39.9	[a].220	.209
			39.9	[a].201	.191
			39.9	[a].230	.220
			39.9	[a].236	.225
			39.9	[a].253	.242
			39.9	[a].237	.227

[a] Signifies wires of length 4.75 mm. All other values obtained with wires of length 5.0 mm.

Turbulence in free tunnel 15.5 feet from rear of honeycomb: $L'=0.303$ inch, $L=0.260$ inch. No noticeable increase with distance was found, although not thoroughly investigated.

TABLE III.—EQUATIONS FOR CURVES OF FIGURE 7

	a	b
¼-inch mesh	$\frac{L}{M}$ = 0.1559	+0.003017 $\frac{x}{M}$
½-inch mesh	$\frac{L}{M}$ = 0.1753	+0.002307 $\frac{x}{M}$
1-inch mesh	$\frac{L}{M}$ = 0.2291	+0.001493 $\frac{x}{M}$
3¼-inch mesh	$\frac{L}{M}$ = 0.1471	+0.002000 $\frac{x}{M}$
5-inch mesh	$\frac{L}{M}$ = 0.1316	+0.002016 $\frac{x}{M}$
All data taken together	$\frac{L}{M}$ = 0.1467	+0.002501 $\frac{x}{M}$

TABLE IV.—INTENSITY OF TURBULENCE

New Data			Old Data		
$\frac{x}{M}$ Distance from screen in mesh lengths	$\frac{(\sqrt{\overline{u^2}})_w}{U}$ (uncorrected)	$\frac{\sqrt{\overline{u^2}}}{U}$ (corrected)	$\frac{x}{M}$ Distance from screen in mesh lengths	$\frac{(\sqrt{\overline{u^2}})_w}{U}$ (uncorrected)	$\frac{\sqrt{\overline{u^2}}}{U}$ (corrected)
¼-inch-mesh screen					
Length of wire, 4.7 mm			Length of wire, 8.4 mm		
16	0.0350	0.0550	48	0.0111	0.0187
24	.0262	.0397	144	.0080	.0110
39	.0188	.0270	288	.0052	.0063
72	.0118	.0156			
100	.0098	.0124			
152	.0084	.0101			
209	.0078	.0090			
284	.0070	.0079			
½-inch-mesh screen					
Length of wire, 4.7 mm			Length of wire, 8.4 mm		
14	0.0411	0.0531	24	0.0189	0.0276
26	.0246	.0310	72	.0096	.0127
46	.0171	.0208	144	.0069	.0084
74	.0120	.0141			
110	.0100	.0114			
163	.0080	.0089			
246	.0064	.0069			
1-inch-mesh screen					
Length of wire, 4.75 mm			Length of wire, 8.4 mm		
25.3	0.0290	0.0324	36	0.0183	0.0218
54.0	.0168	.0185	72	.0122	.0142
85.3	.0117	.0127	108	.0095	.0109
113.3	.0097	.0104			
133.5	.0086	.0092			
164.5	.0073	.0078			

TABLE IV.—INTENSITY OF TURBULENCE—Continued

New Data			Old Data		
$\frac{x}{M}$ Distance from screen in mesh lengths	$\frac{(\sqrt{\overline{u^2}})_w}{U}$ (uncorrected)	$\frac{\sqrt{\overline{u^2}}}{U}$ (corrected)	$\frac{x}{M}$ Distance from screen in mesh lengths	$\frac{(\sqrt{\overline{u^2}})_w}{U}$ (uncorrected)	$\frac{\sqrt{\overline{u^2}}}{U}$ (corrected)
3¼-inch-mesh screen					
Length of wire, 4.7 mm			Length of wire, 8.4 mm		
15.5	0.0434	0.0457	14.8	0.0423	0.0464
20.1	.0341	.0358	25.9	.0270	.0293
27.4	.0253	.0265	36.9	.0204	.0220
37.8	.0210	.0219			
53.8	.0161	.0167			
60.8	.0145	.0150			
5-inch-mesh screen					
Length of wire, 4.7 mm			Length of wire, 8.4 mm		
14.6	0.0470	0.0488	15.4	0.0384	0.0414
21.7	.0336	.0348	26.8	.0254	.0269
29.0	.0260	.0269			
39.4	.0210	.0216			

For the free tunnel, 15.5 feet from the rear of the honeycomb, $\frac{(\sqrt{\overline{u^2}})_w}{U}=0.007$ taken with wire 8.4 mm long. The value corrected for wire length is 0.0085. No noticeable change through the length of the working section of the tunnel was found, although not thoroughly investigated.

TABLE V.—CONSTANTS OF EQUATION (17)

Mesh of screen	$\frac{U}{(\sqrt{\overline{u^2}})_0}$	C_6
¼-inch	0.57	0.483
½-inch	2.81	.516
1-inch	4.28	.577
3¼-inch	2.63	.487
5-inch	1.25	.446

TABLE VI.—CRITICAL REYNOLDS NUMBER OF SPHERES

M Mesh of screen, inches	$\frac{x}{M}$ Distance in mesh lengths	$\frac{100\sqrt{\overline{u^2}}}{U}$ Intensity of turbulence, percent	L Scale of turbulence, inches	5-inch sphere		8.55-inch sphere	
				R_c Critical Reynolds Number	$\frac{100\sqrt{\overline{u^2}}}{U}\left(\frac{D}{L}\right)^{1/5}$	R_c Critical Reynolds Number	$\frac{100\sqrt{\overline{u^2}}}{U}\left(\frac{D}{L}\right)^{1/5}$
5	15.4	4.63	0.813	116,000	6.66	108,000	7.41
5	26.8	2.92	.928	151,000	4.09	145,000	4.55
3.25	14.8	4.55	.574	101,000	7.01	96,000	7.81
3.25	25.9	2.90	.646	142,000	4.37	137,000	4.86
3.25	36.9	2.19	.718	163,000	3.23	159,000	3.59
1	36	2.52	.283	151,000	4.48	134,000	4.98
1	72	1.45	.337	189,000	2.49	178,000	2.77
1	108	1.07	.390	221,000	1.78	215,000	1.98
.5	24	3.39	.115	[a] 129,000	7.21	[a] 116,000	8.03
.5	72	1.48	.171	171,000	2.91	167,000	3.24
.5	144	.94	.254	216,000	1.71	203,000	1.90
.25	48	2.16	.075	[a] 147,000	5.00	[a] 155,000	5.57
.25	144	1.07	.148	190,000	2.16	184,000	2.41
.25	288	.76	.256	240,000	1.38	229,000	1.53
None	----------	.85	.260	268,000	1.54	----------	----------

[a] These values were obtained at a distance of 1 foot from the screen. From figures 16, 17, 18, it is evident that these values are not concordant with the others. See text for discussion.

TABLE VII.—DISTRIBUTION OF VELOCITY PRESSURE q BEHIND SCREENS

M mesh of screen, inches	x/M Distance in mesh lengths	Number of stations	Distance between stations, inches	Number of readings	Approximate speed, ft./sec.	Average ratio of q to wall plate pressure	Maximum deviation from average, percent	Mean deviation from average, percent	Regular pattern present
5	4.8	24	1.0	24	65	0.686	17.7	8.6	Yes
	7.2	23	1.0	23	60	.626	9.3	4.2	Yes
	9.6	24	1.0	24	60	.622	7.4	3.3	Yes
	12.0	42	1.0	42	60	.611	6.0	2.9	No
	14.4	23	1.0	23	60	.614	4.6	2.3	No
					80	.618	4.6	2.3	
	16.8	25	1.0	25	60	.612	4.6	2.2	No
	15.4	60	[a]	120	68	.605	6.0	2.2	No
	26.8	60	[a]	120	68	.618	4.7	2.2	No
3.25	3.69	19	0.5	19	65	.689	27.0	14.5	Yes
	5.54	20	.5	20	60	.648	13.8	6.8	Yes
	7.38	45	.5	45	60	.632	11.2	4.6	Yes
	9.23	42	.5	42	60	.620	6.5	2.6	Yes
		34	.5	34	75	.619	7.0	2.7	
	11.07	22	.5	22	60	.614	5.8	3.1	Yes
	12.92	41	.5	41	60	.596	6.0	3.1	No
	14.76	54	[a]	108	50	.601	6.2	2.9	No
					65	.600	6.2	2.3	
					80	.600	6.6	2.6	
	25.83	54	[a]	108	50	.605	4.7	1.7	No
					65	.606	4.7	1.9	
					80	.603	5.1	2.1	
	36.9	54	[a]	108	50	.618	4.1	1.4	No
					65	.617	4.6	1.7	
					80	.615	5.2	1.8	
1.0	4	23	0.125	23	60	[b].607	15.6	8.7	Yes
	6	26	.125	26	60	[b].680	12.7	5.6	Yes
	8	30	.125	30	60	[b].651	7.4	3.5	Yes
	12	28	.125	28	60	[b].634	2.4	1.2	No
	16	30	.125	30	60	[b].631	2.2	1.3	No
	24	29	.125	29	60	[b].627	1.4	1.1	No
	36	72	[a]	143	35	.622	3.2	.8	No
		72		143	70	.620	2.6	.6	
		60		120	80	.615	2.1	.5	
	72	54	[a]	108	35	.636	2.6	.8	No
					70	.633	1.6	.4	
					80	.627	1.3	.4	
	108	54	[a]	108	35	.646	2.1	.7	No
					70	.644	1.3	.4	
					80	.639	1.5	.4	
0.5	6	23	0.125	23	50	[b].668	13.8	7.7	Yes
	8	23	.125	23	50	[b].637	7.5	4.1	Yes
	10	23	.125	23	50	[b].636	4.9	2.1	Yes
	12	23	.125	23	50	[b].632	4.1	1.8	Yes
	14	23	.125	23	50	[b].631	2.9	1.4	No
	16	23	.125	23	50	[b].630	2.8	1.1	No
	24	60	[a]	120	70	.652	4.0	1.3	No
	72	60	[a]	120	70	.644	2.4	1.0	No
	144	60	[a]	120	70	.641	2.8	.9	No
0.25	4	24	0.063	24	55	[b].790	66.7	28.1	Yes
	6	23	.063	23	55	[b].852	26.6	10.9	Yes
	8	24	.063	24	55	[b].678	19.2	9.7	[c]
	12	24	.063	24	55	[b].594	7.9	4.1	[c]
	16	24	.063	24	55	[b].584	5.1	2.8	[c]
	20	23	.063	23	55	[b].586	3.0	1.4	No
	48	60	[a]	120	70	.614	4.8	1.2	No
	144	60	[a]	120	70	.607	4.9	1.2	No
	288	60	[a]	120	70	.604	3.6	1.0	No

[a] For these positions traverses were made at a number (usually 12) equidistant points along circles of radii 2, 5, 8, 12, and 18 inches from the tunnel axis. At other positions the traverse was made along a line which was parallel to the horizontal wires of the screen and in a horizontal plane passing midway between two wires of the screen.

[b] These traverses were made with a small impact tube, the reference pressure being the wall plate static pressure. The values are approximately but not accurately comparable with values of the velocity pressure.

[c] There was evidence of a regular pattern but the pattern did not correspond to the spacing of the wires of the screens.

TABLE VIII.—FACTORS FOR CORRECTING HOT-WIRE RESULTS FOR EFFECT OF WIRE LENGTH

$\frac{l}{L}$	K_1	K_2
0	1.000	1.000
.4	1.067	1.105
.8	1.133	1.182
1.2	1.198	1.241
1.6	1.263	1.289
2.0	1.327	1.327
2.4	1.390	1.359
2.8	1.451	1.384
3.2	1.512	1.406

TABLE IX.—DISTRIBUTION OF INTENSITY WITH FREQUENCY

[Measurements 26 inches behind 1-inch-mesh screen]

Frequency cycles per second	20 ft./sec.	40 ft./sec.
0–250	0.80	0.65
250–500	.14	.16
500–1500	.05	.16
>1500	.01	.03

TABLE X.—VARIATION OF $\frac{1-R_T'}{1-R_L'}$ WITH FREQUENCY

Measurements 25½ inches behind 1-inch screen with wires 5 mm long and 2 mm apart.

Frequency cycles per second	20 ft./sec.	40 ft./sec.
No filter	1.41	1.37
0–250	2.67	4.89
250–500	1.50	2.50
500–1500	.75	1.40
1500–3000	----------	.83
>3000	----------	.70

U. S. GOVERNMENT PRINTING OFFICE: 1937

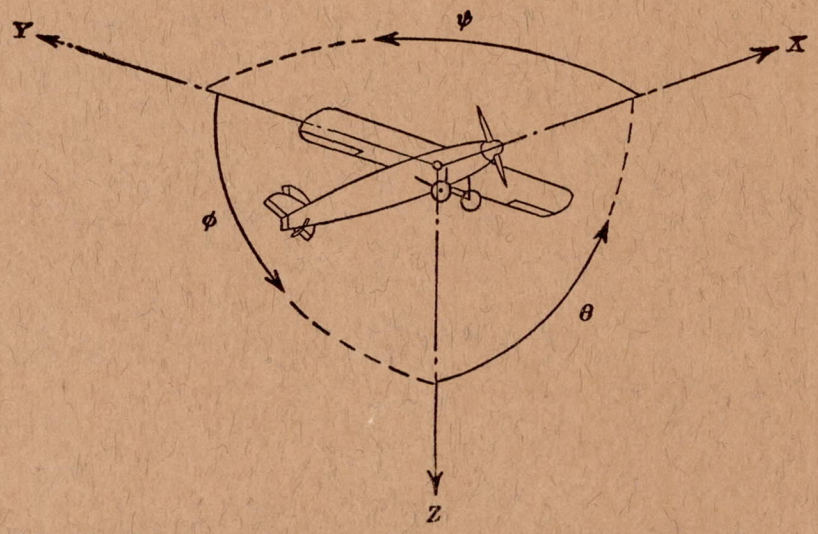

Positive directions of axes and angles (forces and moments) are shown by arrows

Axis		Force (parallel to axis) symbol	Moment about axis			Angle		Velocities	
Designation	Symbol		Designation	Symbol	Positive direction	Designation	Symbol	Linear (component along axis)	Angular
Longitudinal	X	X	Rolling	L	$Y \longrightarrow Z$	Roll	ϕ	u	p
Lateral	Y	Y	Pitching	M	$Z \longrightarrow X$	Pitch	θ	v	q
Normal	Z	Z	Yawing	N	$X \longrightarrow Y$	Yaw	ψ	w	r

Absolute coefficients of moment

$C_l = \frac{L}{qbS}$ (rolling) $\quad C_m = \frac{M}{qcS}$ (pitching) $\quad C_n = \frac{N}{qbS}$ (yawing)

Angle of set of control surface (relative to neutral position), δ. (Indicate surface by proper subscript.)

4. PROPELLER SYMBOLS

D, Diameter

p, Geometric pitch

p/D, Pitch ratio

V', Inflow velocity

V_s, Slipstream velocity

T, Thrust, absolute coefficient $C_T = \frac{T}{\rho n^2 D^4}$

Q, Torque, absolute coefficient $C_Q = \frac{Q}{\rho n^2 D^5}$

P, Power, absolute coefficient $C_P = \frac{P}{\rho n^3 D^5}$

C_s, Speed-power coefficient $= \sqrt[5]{\frac{\rho V^5}{P n^2}}$

η, Efficiency

n, Revolutions per second, r.p.s.

Φ, Effective helix angle $= \tan^{-1}\left(\frac{V}{2\pi r n}\right)$

5. NUMERICAL RELATIONS

1 hp. = 76.04 kg-m/s = 550 ft-lb./sec.
1 metric horsepower = 1.0132 hp.
1 m.p.h. = 0.4470 m.p.s.
1 m.p.s. = 2.2369 m.p.h

1 lb. = 0.4536 kg.
1 kg = 2.2046 lb.
1 mi. = 1,609.35 m = 5,280 ft.
1 m = 3.2808 ft.